C.P. No. 993

C.P. No. 993

MINISTRY OF TECHNOLOGY

AERONAUTICAL RESEARCH COUNCIL

CURRENT PAPERS

The Calculation of Sub-Critical Pressure Distributions on Symmetric Aerofoils at Zero Incidence

By

P. G. Wilby

LONDON: HER MAJESTY'S STATIONERY OFFICE

1968

Price 7s 6d net

C.P. No.993*

March, 1967

The Calculation of Sub-Critical Pressure Distributions on Symmetric Aerofoils at Zero Incidence

- By -

P. G. Wilby

SUMMARY

Several compressibility correction rules that relate the sub-critical velocity on an aerofoil to the incompressible velocity are reviewed. Theoretical and experimental values for velocity at the crest of symmetric aerofoils at zero incidence are studied and a new compressibility correction factor is derived using third-order small disturbance theory. When used in conjunction with the incompressible Weber formula, this new compressibility factor is found to give good agreement with experiment.

* Replaces NPL Aero Report 1208 - A.R.C.28 888

CONTENTS

SYMBOLS

B	general compressibility correction factor.
B_1	particular compressibility correction factor (see Eq.30)
K_1 , K_2	coefficients in second-order expression for compressible flow velocity (defined by Eqs. 16,17 and 18).
k_1 , k_2 , k_3	coefficients in third-order expression for compressible flow velocity (defined by Eq.27).
M	Mach number.
n =	$\frac{\gamma+1}{2}\frac{M^2}{\beta^2}$.
$S^{(1)}(x)$	thickness term in Weber formula for velocity on an aerofoil (see Ref.5).
U	non-dimensional total velocity $(=1+u)$.
u	non-dimensional perturbation velocity.
u_1	first-order perturbation velocity.
u_2	second-order contribution to perturbation velocity.
u_3	third-order contribution to perturbation velocity.
p	static pressure.
ρ	density.
C_p	pressure coefficient $\left(= \frac{p-p_\infty}{\frac{1}{2}\rho_\infty u_\infty^2} \right)$.
x, z	rectangular cartesian co-ordinates, x measured in free stream direction.
β =	$\sqrt{1-M_\infty^2}$
γ	ratio of specific heats of air (taken to be 1.4).
λ	parameter that defines B .
λ_1 , λ_2	coefficients in third-order solution for λ (see Eq.28).
ϕ	perturbation velocity potential function.
ϕ_1 , ϕ_2	first- and second-order contributions to ϕ .
r	axis ratio of an ellipse.

Subscripts

∞	free stream conditions.
i	incompressible-flow value.

1. Introduction

It is useful first to outline the dominant changes that occur in an aerofoil pressure distribution as Mach number increases. Over the major part of the aerofoil surface, where the slope is small, the pressure decreases as Mach number increases; a region of supersonic flow eventually develops and is usually terminated by a shock wave. This overall effect is illustrated in Fig. 1., which shows experimental pressure distributions for a NACA 0012 aerofoil at zero incidence. The reduction of pressure as Mach number increases is predicted by small disturbance theory, which shows that the perturbation velocity at the surface can be obtained by applying a Mach-number dependent compressibility factor to the perturbation velocity for incompressible flow. The accuracy of the theoretical results, in the region of small surface slope, depends more upon the order of accuracy of the theory that is built on the basic assumption of small disturbance than upon the basic assumption itself.

In the region of large surface slope, the situation is somewhat different, as here the pressure increases as Mach number increases. Obviously, at some intermediate value of slope there must be a neutral point where the pressure for some free stream velocity is the same as for the incompressible case. If it were possible in this region to express the perturbation velocity simply as a compressibility correction applied to the incompressible value, then there would be one single neutral point for all values of free stream Mach number. This common neutral point would of course be the point at which the perturbation velocity was zero (i.e. where the pressure coefficient $C_p = o$). That this is not so is evident in Fig. 2., which shows that pairs of pressure distributions intersect at different points, and that the neutral point varies with Mach number. Thus it is evidently not sufficient to apply a compressibility factor to an accurate incompressible perturbation velocity, but for realistic results some allowance must be made for the way in which the influence of surface slope varies with Mach number.

Apart from the compressibility effects that are associated with a symmetric aerofoil at zero incidence, the manner in which camber and incidence induced velocities vary with Mach number should also be studied. This, however, must be deferred until better data are available for assessing the results. No exact theoretical solutions are so far available and the use of experimental data is complicated by the viscous effects on circulation - which arise from the fact that the differential boundary-layer growth on the two surfaces distorts the effective camber and incidence. For the present, therefore, attention will be confined to thickness-induced perturbation velocities as deduced for symmetrical aerofoils at zero incidence, for which the significant effects of boundary layer growth are confined to the rear part of the aerofoil.

The theories that will be discussed here are based on the isentropic equations of motion and cannot be called upon to represent flows that include a region of supersonic velocity with a terminating shock wave. Thus, in the main, only sub-critical flows will be considered.

Several existing compressibility correction rules will be reviewed and their results compared with experiment at the crests of various aerofoils. It will be shown that none of these rules can be considered accurate for the whole range of sub-critical Mach numbers, and that there is a need for an improved theory. With the intention of satisfying this need, a compressibility correction based on third-order theory will be presented and the resulting theoretical pressure distributions compared with experiment. In the derivation of this correction, particular emphasis is placed on its incorporation within the framework of the Weber formula because this is so convenient and so widely used.

2. Compressibility Correction Laws

2.1. Prandtl-Glauert Law

Glauert[1] and Prandtl[2] derived an expression for the compressible perturbation velocity from the linearised form of the velocity potential equation,

$$(1-M_\infty^2)\,\phi_{xx} + \phi_{zz} = 0 \qquad (1)$$

Their solution of this equation gives the perturbation velocity u in the free stream direction as

$$u = \frac{1}{\beta}\, u_i \quad ,$$

where

$$\beta = \sqrt{1-M_\infty^2} \quad , \qquad (2)$$

and the suffix denotes the incompressible value. This being a small perturbation theory, transverse velocity perturbations are neglected and the non-dimensional disturbed total velocity is given as

$$U = 1 + u \, .$$

Although derived as a velocity rule, the Prandtl-Glauert Law is usually used in its pressure coefficient form

$$C_p = \frac{1}{\beta}\; C_{p_i} \quad , \qquad (3)$$

which comes from substituting Eq. 2 in the linearised expression for C_p.

Due to the approximations involved, this law is valid only for thin aerofoils at low subsonic Mach numbers.

2.2. Kármán-Tsien Law

The Kármán-Tsien Law was originally derived[3] using the hodograph method which produces a pressure law,

$$C_p = \frac{C_{p_i}}{\beta + \frac{1}{2}(1-\beta)C_{p_i}} \qquad (4)$$

Spreiter[4] shows that this result can also be derived from the velocity potential equation if it is written in the simplified second-order form;

$$(1-M^2)\,\phi_{xx} + \phi_{zz} = 0 \, , \qquad (5)$$

where M is the local Mach number. On setting $\gamma = -1$, a simplified

/expression

expression for M in terms of M_∞ leads to the solution

$$u = \frac{u_1}{\beta-(1-\beta)u_1} \quad .$$

Substitution of this in the linearised equation for C_p gives the usual pressure law of Eq. 4. It should, however, be noted that the above velocity rule used in conjunction with the exact expression for C_p gives a less accurate result than Eq.4.

2.3. Spreiter's Law

A slightly more rigorous solution of Eq. 5 is presented by Spreiter and Alksne [4], but again a simplifying assumption is made. The local Mach number M is expressed in terms of M_∞ and Eq. 5 becomes

$$\left[1-M_\infty^2-(\gamma+1)M_\infty^2\,\phi_x\right]\phi_{xx}+\phi_{zz} = 0 \qquad (6)$$

The coefficient of ϕ_{xx} is temporarily assumed constant to give

$$u = \frac{u_i}{\sqrt{1-M_\infty^2-(\gamma+1)M_\infty^2\,u}} \quad , \qquad (7)$$

and with the same assumption maintained, Eq. 7 is differentiated with respect to x. The resulting equation is then treated as a non-linear differential equation in u, which is solved to give

$$u = \frac{1}{(\gamma+1)M_\infty^2}\left\{\beta^2-\left[\beta^3-\frac{3}{2}(\gamma+1)\,M_\infty^2\,u_i\right]^{2/3}\right\} \qquad (8)$$

Using the linearised equation for C_p, this gives

$$C_p = -\frac{2}{(\gamma+1)M_\infty^2}\left\{\beta^2-\left[\beta^3+\frac{3}{4}(\gamma+1)\,M_\infty^2\,C_{p_i}\right]^{2/3}\right\} \qquad (9)$$

This theory does not give real results for velocities greater than the predicted critical value and is not reliable for velocities that are just sub-critical.

2.4. Küchemann-Weber Formula

Küchemann and Weber[6] derive a compressibility factor that can be applied to the incompressible solution for velocity on an aerofoil, as given by Weber [7]. They start with Eq. 4 and obtain an approximate expression for local Mach number so that the velocity potential equation can be written,

$/ \left[1-M_\infty^2\right.$ ....

$$\left[1-M_\infty^2(1+2\,\phi_x)\right]\ \phi_{xx} + \phi_{zz} = 0 \tag{10}$$

This is seen to be the equation solved by Spreiter, when $\gamma=1$.

In order to obtain a simple solution to Eq. 10, the coefficient of ϕ_{xx} must be constant and this condition is satisfied by writing

$$2\,\phi_x = -\,C_{p_1} \quad ,$$

where C_{p_1} is taken to be some suitable mean value. The solution then follows the same arguments as the first order solution and gives the perturbation velocity as

$$u = \frac{u_1}{\sqrt{1-M_\infty^2(1-C_{p_1})}} \quad .$$

If the compressibility factor found in this equation is applied to all terms in the incompressible Weber formula (Ref. 5) that involve z, then the velocity on a symmetric aerofoil at zero incidence is,

$$U = \frac{1}{\sqrt{1+\left(\frac{1}{B}\frac{dz}{dx}\right)^2}}\left[1 + \frac{S^{(1)}(x)}{B}\right] \quad , \tag{11}$$

$$\text{where} \quad B = \sqrt{1-M_\infty^2(1-C_{p_1})} \quad , \tag{12}$$

and $S^{(1)}$ is a function of the thickness distribution. Usually the local value of C_{p_1} is used rather than a constant mean value and it is suggested that B should be taken to be β when $C_p > 0$. Finally, the pressure coefficient C_p is calculated by substituting Eq. 11 in the exact isentropic expression

$$C_p = \frac{2}{\gamma M_\infty^2}\left\{\left[1 + \frac{\gamma-1}{2} M_\infty^2(1-U^2)\right]^{\frac{\gamma}{\gamma+1}} - 1\right\} \quad .$$

This is the first theoretical result that allows for the manner in which the non-linear influence of surface slope varies with Mach number, and which was shown above to be a pre-requisite for accurate results.

/2.5.

2.5. Second-Order Theory

Suppose that the velocity potential function is expressed as the sum of the first-order solution and a second-order term, that is

$$\phi = \phi_1 + \phi_2 \quad . \tag{13}$$

The first-order solution ϕ_1 is obtained by solving the first-order potential equation with boundary conditions satisfied on the $z = o$ plane, but to find the second-order term it is necessary to solve the second-order potential equation with boundary conditions satisfied on the aerofoil surface. Because of these differences in procedure, the compressibility correction to the second-order term will differ from that applicable to the first-order solution. Expressing the velocity potential in the form of Eq. 13, Hayes (7) solves the equation

$$(1-M_\infty^2)\phi_{xx} + \phi_{zz} = \frac{\gamma+1}{2} M_\infty^4 (\phi_x)^2_x + M_\infty^2 \left[\phi_z^2 + (1-M_\infty^2)\phi_x^2\right], \tag{14}$$

which includes all the second-order terms of the full potential equation. Hayes then shows that the ratio of the second-order term to the first-order term, for velocity on the surface of an aerofoil, is

$$\frac{t}{(1-M_\infty^2)^{3/2}} \left[\frac{\gamma+1}{2} M_\infty^4 + 2(1-M_\infty^2)\right] ,$$

where t is a measure of the aerofoil thickness.

This result is used by Van Dyke(8) who shows that if the incompressible velocity is given by

$$U_i = 1 + u_1 + u_2 \; , \tag{15}$$

where u_1 contains linear terms in thickness, camber and incidence, and u_2 their squares and products, then in compressible flow the velocity is

$$U = 1 + K_1 u_1 + K_2 u_2 + \frac{K_2 - 1}{2} u_1^2 \; , \tag{16}$$

where $K_1 = \dfrac{1}{\beta}$ (17)

and $K_2 = \dfrac{(\gamma+1) M_\infty^4 + 4\beta^2}{4\beta^4}$ (18)

This second-order solution is the most rigorous of the theories so far discussed, with its accuracy dependent only upon the convergence of the series solution for velocity.

3. Velocity at Aerofoil Crest

3.1. Assessment of Second-Order Solutions

The crest of an aerofoil is the point at which the tangent to the surface is parallel to the free stream direction, and for a symmetric aerofoil this is the point of maximum thickness and zero surface slope. The velocity at the crest forms a convenient basis for the comparison and assessment of existing correction factors - and the initial derivation of an improved factor - because the terms related explicitly to surface slope disappear there. These latter terms are of course very important and must be considered at some stage of the assessment of a compressibility correction rule.

Each of the laws discussed in the previous section provides a different expression for crest velocity as follows:

Prandtl-Glavert $$U = 1 + \frac{u_i}{\beta} \tag{19}$$

Karman-Trien $$U = 1 + \frac{u_i}{\beta-(1-\beta)u_i} \tag{20}$$

Spreiter $$U = 1 + \frac{\beta^2 - [\beta^3 - \frac{3}{2}(\gamma+1)\, M_\infty^2\, u_i\,]^{2/3}}{(\gamma+1)\, M_\infty^2} \tag{21}$$

Küchemann-Weber $$U = 1 + \frac{u_i}{\sqrt{1-M_\infty^2(1-C_{p_i})}} \tag{22}$$

Van Dyke $$U = 1 + \frac{u_i}{\beta} + \frac{(1-0.4\, M_\infty^2)}{2\beta^4}\, M_\infty^2\, u_i^2 \tag{23}$$

Eq. 23 comes directly from Eq. 16 if it is assumed that $u_2 = 0$. This is exactly true for an ellipse and in general u_2 is found to be negligibly small, even compared with u_1^2, for most practical section shapes; this explains the high accuracy of the Weber formula (5) for incompressible flow. Thus, if will be assumed that Eq. 23, which is certainly valid at the crest of an ellipse, is valid also at the crest of a general symmetric aerofoil.

Now Van Dyke's solution can be thought of as the first three terms of a series in ascending powers of u_i, and if Eq. 23 is re-arranged to give

$$U = 1 + \frac{u_i}{\beta}\left[1 + \frac{(1-0.4\, M_\infty^2)}{2\beta^3}\, M_\infty^2\quad u_i\right] ,$$

then the terms in the square brackets are the first two terms of a power series in u_i. As

$$\frac{(1-0.4\, M_\infty^2)}{\beta^3}\, M_\infty^2\quad u_i$$

is small compared with unity they can, to second order, be replaced by

$$\left[1 - (1-0.4\, M_\infty^2)\,\frac{M_\infty^2}{\beta^3}\quad u_i\right]^{-\frac{1}{2}} ,$$

/The

The velocity can thus be written in the form

$$U = 1 + \frac{u_i}{B} , \tag{24}$$

where
$$B = \sqrt{1-M_\infty^2(1 + \lambda_1 u_i)} \tag{25}$$

and
$$\lambda_1 = \frac{1-0.4 M_\infty^2}{\beta} \tag{26}$$

The second-order solution is now expressed in the same form as Eqs. 19, 20 and 22, making possible a direct comparison of existing compressibility correction factors.

As a check on the approximations made in going from Eq. 23 to Eq. 24, values of velocity given by these two equations are compared in Fig. 3 for the particular case of $u_i = 0.2$. (This, of course, is equivalent to the crest velocity on a 20% thick ellipse). Included in the figure are the results given by Kármán-Tsien (Eq. 20) which is an approximate second-order solution. It is seen that the Kármán-Tsien velocity is close to the Van Dyke solution but a little below, and that Eq. 24 gives velocities that are slightly higher than the Van Dyke solution. The latter observation indicates that the third and higher order terms implied by Eqs. 24 and 25 are very small.

In Fig. 4 the second-order result (Eqs. 24 to 26) is compared with Spreiter (Eq. 21) and Küchemann-Weber (Eq. 22). The two latter laws are found to agree fairly well until just below the critical Mach number, and both give considerably higher values of velocity than those given by second-order theory. That such significant differences can occur points fairly clearly to the need to examine a third-order solution.

3.2. A Third-Order Solution

A third-order solution is given by Hantzsche[9] for the maximum velocity on an ellipse at zero incidence. If the axis ratio of the ellipse is τ then $u_i = \tau$ and Hantzsche shows that the compressible velocity is given by

$$U = 1 + k_1 u_i + k_2 u_i^2 + k_3 u_i^3 , \tag{27}$$

where
$$k_1 = \frac{1}{\beta} ,$$

$$k_2 = \frac{(1-0.4 M_\infty^2)}{2\beta^4} M_\infty^2 ,$$

and
$$k_3 = \frac{M_\infty^2}{\beta^3}\left\{\frac{\pi}{4}\left[1 + \frac{n}{4}\left(1+\frac{n}{2}\right)(8-M_\infty^2) - \left(\frac{1}{2} + \frac{3}{4}n + \frac{1}{3}n^2\right)\right]\right\} ,$$

with
$$n = \frac{\gamma+1}{2}\frac{M_\infty^2}{\beta^2}$$

/It

It is seen that the first three terms of Eq. 27 give Van Dyke's second-order solution (Eq. 23) which, it has been argued, can be assumed to be valid at the crest of a general symmetric aerofoil, and it will be assumed here that the third-order term in Eq. 27 is also valid for a general symmetric aerofoil. Thus, Eq. 27 will be taken to be the third-order solution for the velocity at the crest of a symmetric aerofoil.

Now it would be convenient if it were possible to rearrange Eq. 27, in the same way as was done for the second-order solution, to the form of Eq. 24. To do this, we require the expansion of $\frac{u_1}{B}$ to give not only the correct first and second-order terms but also the correct third-order term. This can be achieved by writing

$$B = \sqrt{1-M_\infty^2\left[1+\lambda_1\left(1+\lambda_2 u_1\right)u_1\right]}\ , \tag{28}$$

where λ_2 will be given by equating the coefficients of u_1^3, in the expansion of $\frac{u_1}{B}$, to k_3. It is found that

$$\lambda_2 = \frac{k_3}{k_2} - \frac{3}{2}\beta\ k_2 \ .$$

Values of the coefficients k_1, k_2, k_3, λ_1 and λ_2 are tabulated in Table 1 for various values of Mach number.

The only limitation on the accuracy of this third-order solution is set by the convergence of the series that is used to express velocity. In Fig. 5 the first, second and third-order solutions are plotted against M_∞ for several values of u_i and it is seen that the results converge quickly at low to moderate sub-critical Mach numbers. Convergence becomes less rapid as critical Mach number is approached and eventually breaks down in the super-critical region. As a result of this rather slower rate of convergence near critical conditions there is probably a further advantage, in addition to convenience, in expressing velocity according to Eqs. 24 and 28 as the implied fourth and higher-order terms may give improved accuracy. The effect of these extra terms on the predicted velocity is shown in Fig. 5.

In Figs. 6, 7, 8 and 9, experimental values of crest pressures are compared with second and third-order theory and with Küchemann-Weber theory for four different aerofoils. The experimental results for NACA 0015 section were taken from Ref. 10 and the results for the other three sections are from unpublished NPL results. All cases show very good agreement between third-order theory and experiment, and also show that the Küchemann-Weber correction tends to overestimate velocity. The other compressibility correction that is widely used is the Kármán-Tsien rule which gives results that are very close to second-order theory (see Fig. 3) which agrees well with experiment in the lower Mach number range but underestimates velocity at the higher Mach numbers.

3.3. Simplified Representation of Third-Order Theory

For convenience we will write the compressibility correction as

$$B = \sqrt{1-M_\infty^2 (1 + \lambda u_1)} \quad , \qquad (29)$$

with $\lambda = \lambda_1(1+\lambda_2 u_1)$ being the third-order solution. This expression for λ is rather complicated for use in quick computation and a simplified expression would be much more convenient.

At an early stage in this investigation of compressibility corrections it was found empirically that good results were given by using the factor

$$B = B_1 = \sqrt{1-M_\infty^2 (1-M_\infty C_{p_1})} \quad . \qquad (30)$$

This is equivalent to putting

$$\lambda = -M_\infty \frac{C_{p_1}}{u_1} \quad ,$$

in Eq. 29, and this expression for λ is compared with others in Fig. 10. Remembering that the Prandtl-Glauert rule is equivalent to $\lambda = 0$, that the Küchemann-Weber rule is equivalent to $\lambda = -\frac{C_{p_1}}{u_i} (\simeq 2)$, and that the results given by these two rules differ by a very small amount when Mach number is less than 0.4, we see from Fig. 10 why this empirical expression was found to work so well, and why it can be used as a simple approximation to the third-order solution. It will be realized that for $M < 0.4$ a variation of λ between the values 0 and 2 produces only very small changes in the value for velocity and that the exact value of λ (provided it lies between 0 and 2) is thus of little importance in this low Mach number range.

Aerofoil crest pressure coefficients that are obtained when Eq. 30 is used as the compressibility correction are shown in Figs. 6 and 7, and are seen to differ from those given by Eqs 24 and 28 only at supercritical Mach numbers. For the cases illustrated in Figs. 8 and 9, the use of Eq. 30 produced a negligible difference for Mach numbers below 0.8. Thus, Eq. 30 seems to provide an acceptable simplification for sub-critical Mach numbers.

4. Application of Simplified Third-Order Law to Complete Velocity Distributions

For a symmetric aerofoil at zero incidence in incompressible flow, Weber[5] gives the velocity on the aerofoil surface as

$$U_1 = \frac{1}{\sqrt{1+\left(\frac{dz}{dx}\right)^2}} \left[1 + S^{(1)}(x) \right] \qquad (31)$$

/where

where $S^{(1)}(x)$ is a function of the aerofoil thickness distribution. This formula has proved extremely flexible and is widely used, for example, in the direct aerofoil design problem, in methods for incorporating viscous effects in aerofoil velocity prediction, and in prediction and design methods for swept wings. It is thus desirable to incorporate the revised compressibility correction into this equation for the velocity at all points on the aerofoil.

In order to simplify the argument we will again consider the case of an ellipse whose axis ratio is τ. Over the major part of the chord the surface slope $\frac{dz}{dx}$ is small and Eq. 31 can be written approximately as

$$U_i = (1 + \tau)\left[1 - \frac{1}{2}\left(\frac{dz}{dx}\right)^2 + \ldots\ldots\right]$$

$$= (1 + \tau)\left[1 - \frac{1}{2}\,\frac{\tau^2}{4x}\,\frac{(2x-1)^2}{(1-x)} + \ldots\ldots\right]$$

$$= 1 + \tau - \frac{1}{8}\,\frac{(2x-1)^2}{x(1-x)}\,\tau^2 \quad , \tag{32}$$

if terms that are of third-order in τ are ignored. Following Van Dyke's second-order compressible flow theory, the compressible velocity can now be written as

$$U = 1 + K_1\,\tau + \frac{K_2 - 1}{2}\,\tau^2 - K_2\,\frac{(2x-1)^2}{8x(1-x)}\,\tau^2 \ . \tag{33}$$

Suppose now that we wish to express the compressible velocity in the form

$$U = \frac{1}{\sqrt{1 + \left(\frac{1}{B_2}\frac{dz}{dx}\right)^2}}\left[1 + \frac{\tau}{B_1}\right] \quad , \tag{34}$$

i.e.

$$U = 1 + \frac{\tau}{B_1} - \frac{1}{8}\,\frac{(2x-1)^2}{x(1-x)}\,\frac{\tau^2}{B_2^{\,2}} \quad \text{approx.} \tag{35}$$

Now we have seen that the first three terms of Eq. 33 are represented by the first two terms of Eq. 35 if B_1 is given by Eq. 25, or even better, by the third-order result in Eq. 28. Thus, comparing Eqs. 33 and 35 we have that

$$B_2^{\,2} = \frac{1}{K_2} \ . \tag{36}$$

It has been general practice, when using the Küchemann-Weber formula, to take B_2 and B_1 to be the same (both given by Eq. 12). This is based on the principle that the formula gives the velocity in incompressible flow on the surface of an aerofoil whose ordinates are those of the aerofoil in question divided by the compressibility factor. Thus, any term that is linear in z is divided by the correction factor B (see Ref. 6). From the practical point of view, it is much more convenient to be able to use the

/same

same compressibility factor throughout the equation, and with this possibility in mind $\sqrt{\frac{1}{K_2}}$ is compared with B_1 in Fig. 12, for various values of C_{p_1}, over the range of Mach number that is of interest. The chosen values of C_{p_1} correspond to certain points on the surface of a 15% thick ellipse, and thus help to show that B_1 and B_2 are very close in value in the region for which the derivation of B_2 is valid (that is, the region of small surface slope). Thus, for the major part of an aerofoil surface we can, in fact, take B_2 to be equal to B_1.

In the absence of a valid theoretical solution for the region of large surface slope we will put $B_2 = B_1$ everywhere and compare the resulting theoretical results with experiment. Such a comparison is made in Fig. 3 for the leading-edge of a 10% thick elliptic aerofoil, and velocity is plotted there against surface slope. It is seen that the use of the same factor for slope term and thickness term gives good agreement with experiment, and that even better agreement is obtained when B is put equal to β for $C_{p_1} > 0$. This is a procedure that is recommended for the Küchemann-Weber formula.

If we again assume that what is valid for an ellipse is also valid for a general symmetric aerofoil, then we can write the velocity on the aerofoil surface as

$$U = \frac{1}{\sqrt{1 + \left(\frac{1}{B}\frac{dz}{dx}\right)^2}} \left[1 + \frac{S^{(1)}(x)}{B}\right] , \tag{37}$$

$$\text{where } B = \begin{cases} \sqrt{1 - M_\infty^2 (1 + \lambda u_i)} & \text{for } u_i > 0 \\ \sqrt{1 - M_\infty^2} & \text{for } u_i < 0 . \end{cases}$$

A procedure for calculating the function $S^{(1)}(x)$ is given by Weber (Ref. 5).

Pressure distributions for four aerofoils at zero incidence are shown in Figs. 14, 15, 16 and 17. The first two aerofoils are Nieuwland aerofoils, and his exact theoretical solutions are compared with those obtained from Eq. 37. For the third and fourth cases, theory is compared with experiment. It is seen in each case that Eq. 37 gives very good results when

$$\lambda = - M_\infty \frac{C_{p_1}}{u_1} ,$$

$$\text{or } B = B_1 = \sqrt{1-M_\infty^2(1-M_\infty C_{p_1})} . \tag{38}$$

The Nieuwland aerofoils do not have entirely sub-critical pressure distributions as they have regions of local supersonic flow. However, they are calculated to have isentropic compressions in inviscid flow at the particular Mach numbers indicated in the figures, and thus give a good

/basis

basis for comparison with the present approximate theory. A further point concerning the second Nieuwland aerofoil is that this has an unusually thick leading-edge and it is suspected that the incompressible Weber formula will overestimate velocity near the leading edge. Any such errors will of course be magnified in the pressure distributions of Fig. 15.

5. Conclusions

Of the methods for calculating aerofoil velocity distributions that have been considered here, the most accurate is a compressible form of the Weber formula (Eq. 37), with a compressibility correction based on third-order theory. Third-order theory provides the compressibility factor given in Eq. 28, but for most practical purposes this can be replaced by the simplified factor given in Eq. 30.

Attention has been restricted here to the case of symmetric aerofoils at zero incidence, but the effect of compressibility on the contributions to velocity due to camber and incidence are being considered in order to extend the study to lifting aerofoils.

BMG

REFERENCES

1. H. Glauert — The effect of compressibility on the lift of an aerofoil. Proc.Roy.Soc.A, Vol.118 p.113-9, 1928.

2. L. Prandtl — Über Strömungen deren Gerschwindigkeiten mit der Schallgechwindigkeit vergleichbar sind. J.Aero.Res.Inst.Tokyo. Vol.65, 1930.

3. Th. von Kármán — Compressibility effects in aerodynamics. J.Aero.Sci. 8, 337-356 (1941).

4. J. R. Sprieter, A. Y. Alksne — Thin aerofoil theory based on approximate solution of the transonic flow equation. NACA Report 1359, 1958.

5. J. Weber — The calculation of the pressure distribution over the surface of two-dimensional and swept wings with symmetrical aerofoil sections. R & M No. 2918, July, 1953.

6. D. Küchemann, J. Weber — The subsonic flow past swept wings at zero lift without and with body. R & M No. 2908, 1956.

7. D. W. Hayes — Second-order pressure law for two-dimensional compressible flow. J. Aero.Sc., April, 1955.

8. M. D. Van Dyke — Second-order subsonic aerofoil theory including edge effects. NACA Report 1274, 1956.

9. W. Hantzsche — Die Prandtl-Clauertsche Näherung als Grundlage für ein Iterationsverfahren zur Berechnung kompressibler Unterschallströmungen. Z.angew.Math.Mech., Bd.23, 1943, pp.185-199.

10. D. J. Graham, G. E. Nitzberg and R. N. Olson — A systematic investigation of pressure distributions at high speeds over five representative NACA low-drag and conventional airfoil sections. NACA Report 832.

11. G. Y. Nieuwland — The computation by Lighthill's method of transonic potential flow around a family of quasi-elliptical aerofoils. NLR Report NLR-TR T.83, Amsterdam Sept. 1964. A.R.C.26 609.

M	$\frac{1}{\beta}$	k_2	k_3	λ_1	λ_2
.4	1.09	.105	.101	1.020	0.856
.5	1.155	.200	.255	1.035	1.015
.6	1.250	.375	.696	1.070	1.41
.7	1.400	.760	2.21	1.123	2.10
.8	1.667	1.825	10.55	1.24	4.14

TABLE 1. COEFFICIENTS IN THIRD-ORDER VELOCITY EQUATIONS

FIG. 1

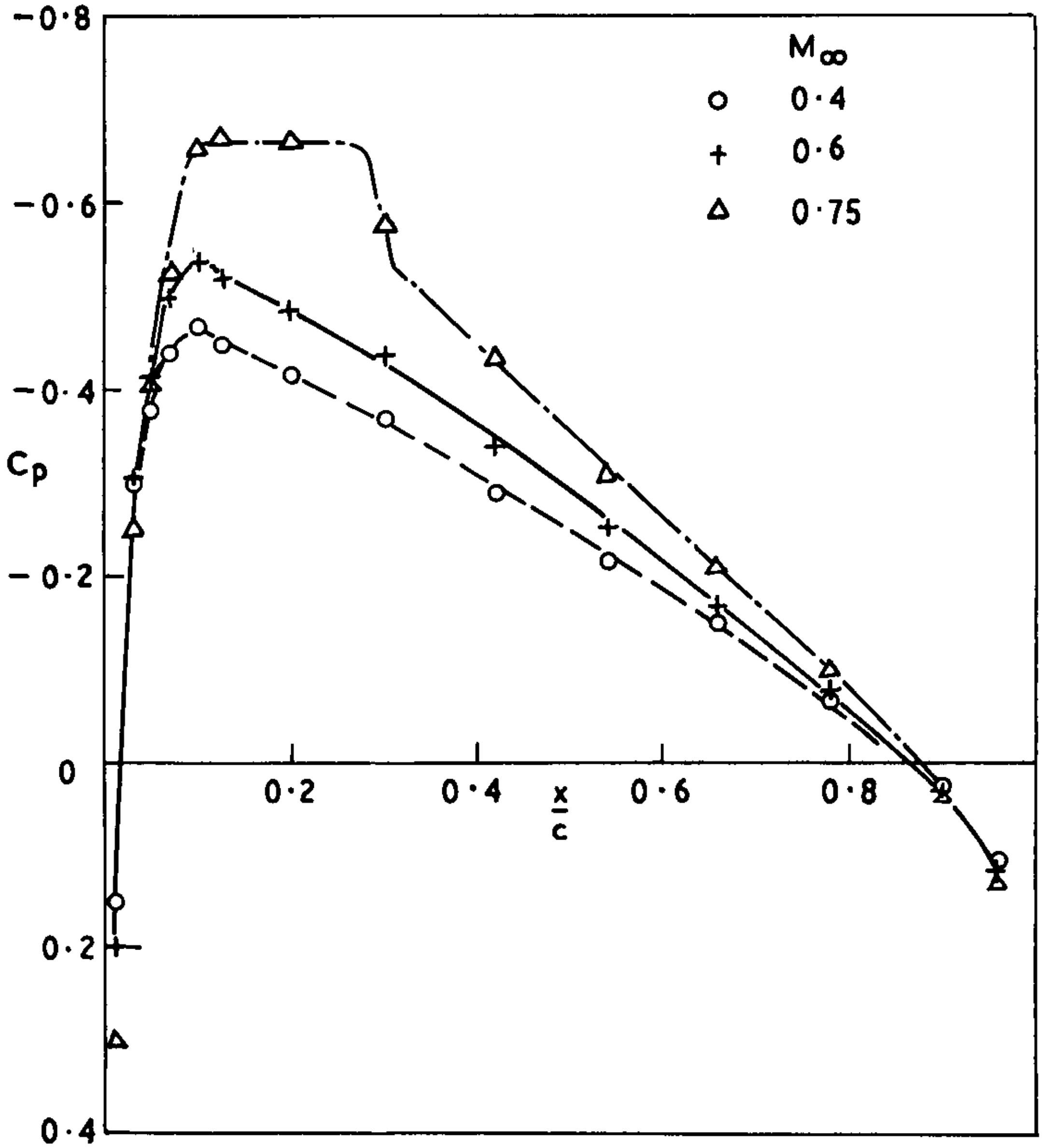

Experimental pressure distributions on NACA 0012 aerofoil

FIG. 2

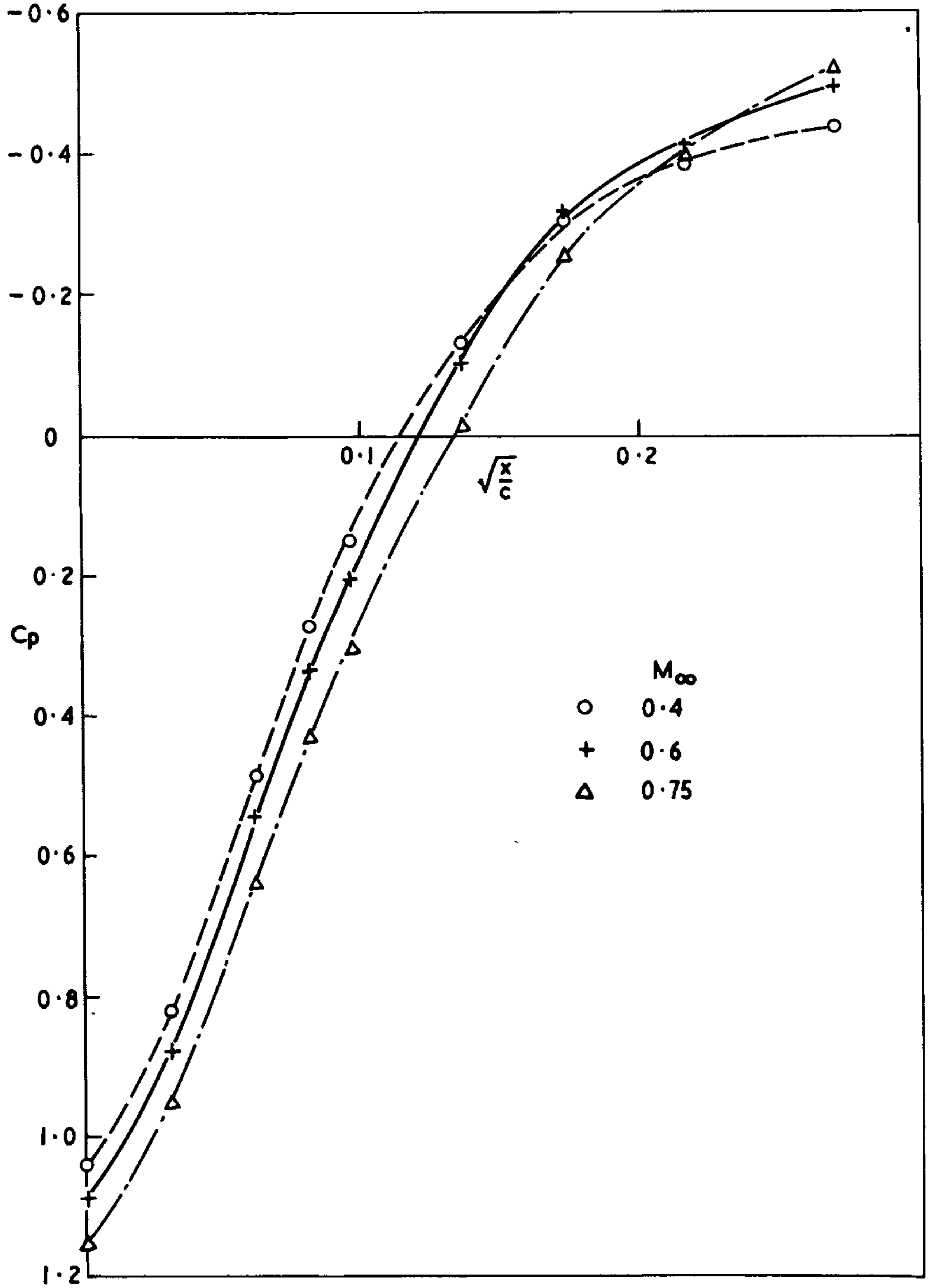

Experimental pressure distribution on leading edge of NACA 0012 aerofoil

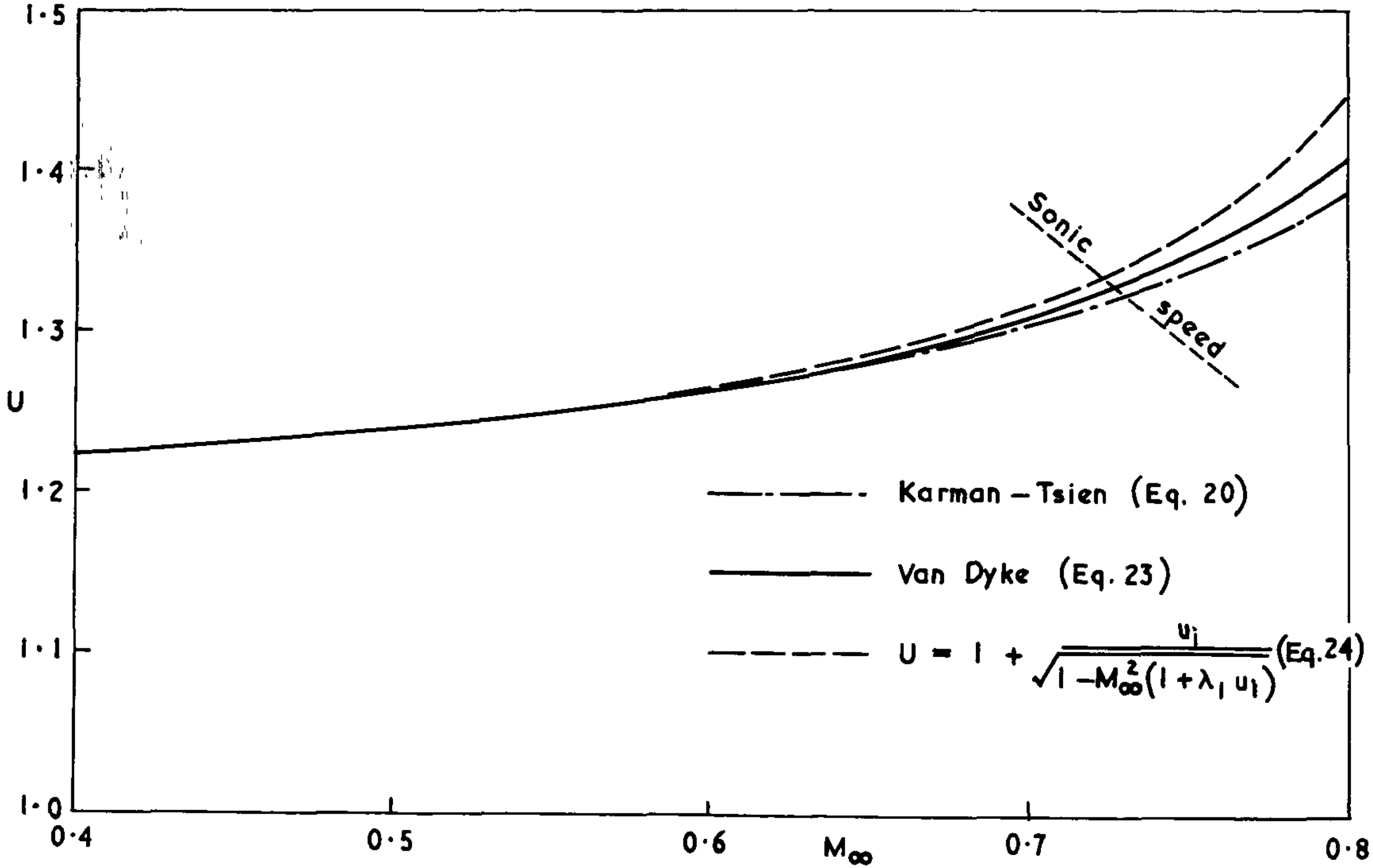

Comparison of second-order theories for $U_i = 1 \cdot 2$

FIG. 3

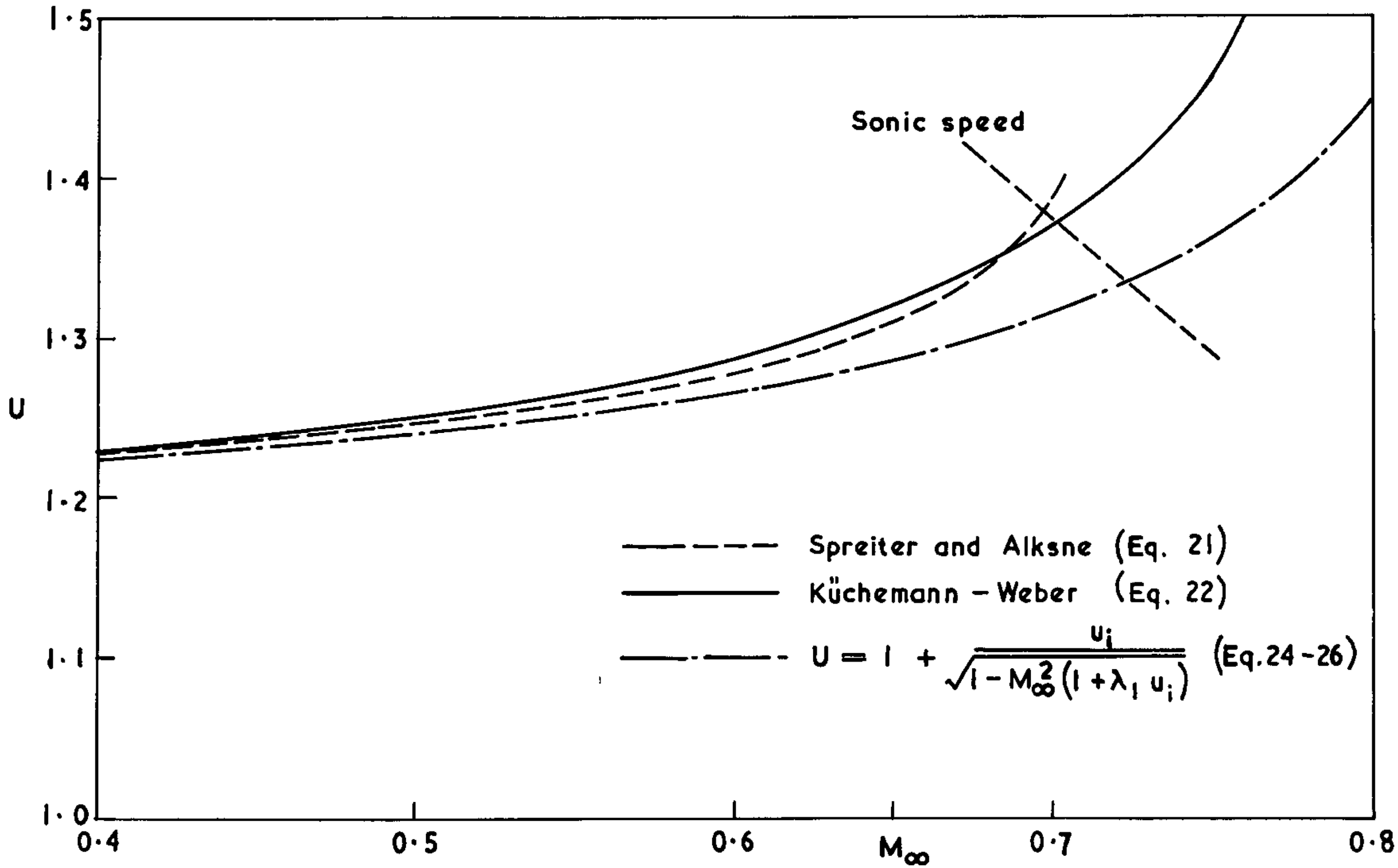

Comparison of compressible velocity laws $U_i = 1{\cdot}2$

FIG. 4.

FIG. 5

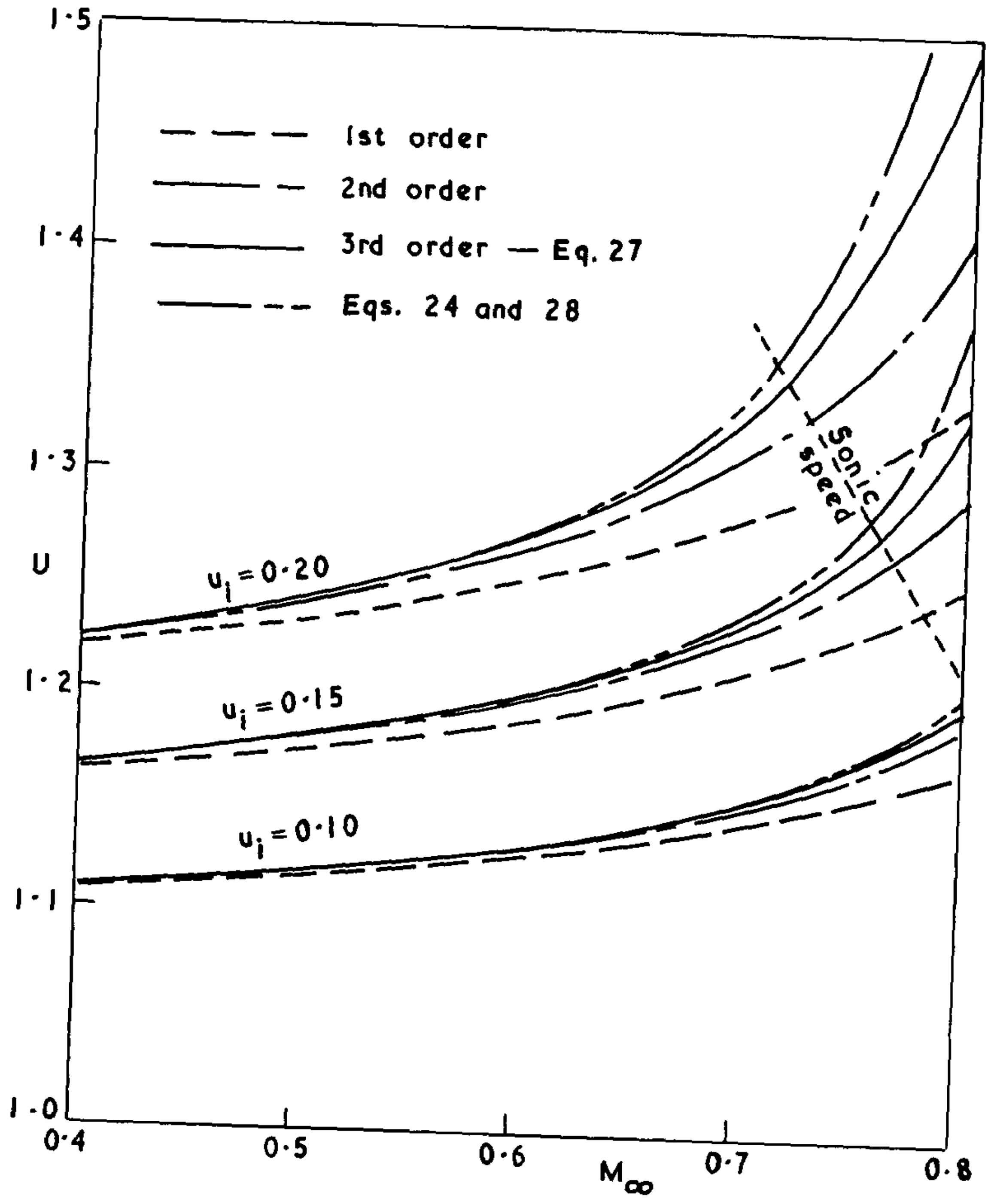

Convergence of third order series solution

FIG. 6

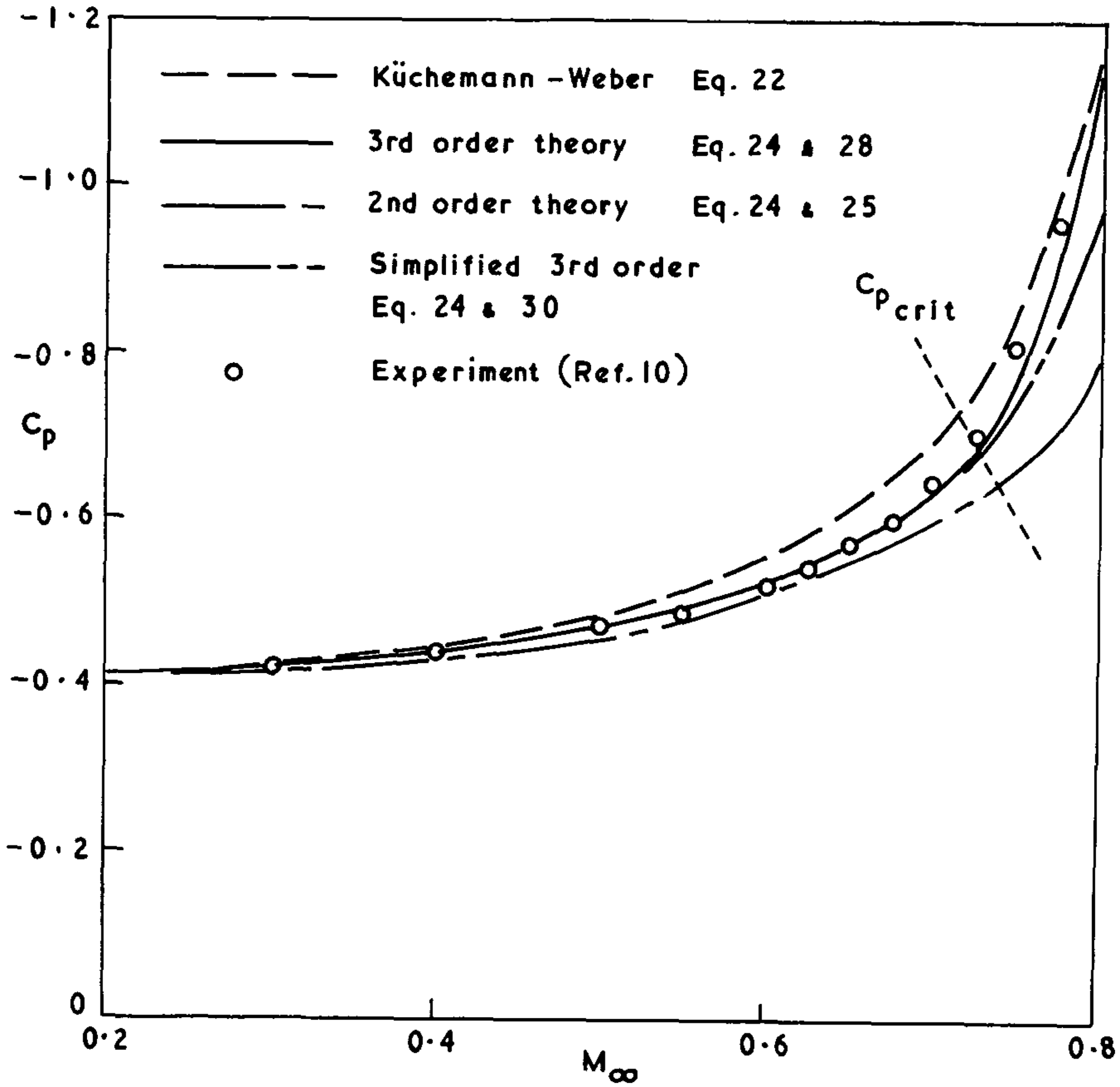

Pressure at crest of a NACA 0015 aerofoil

FIG.7

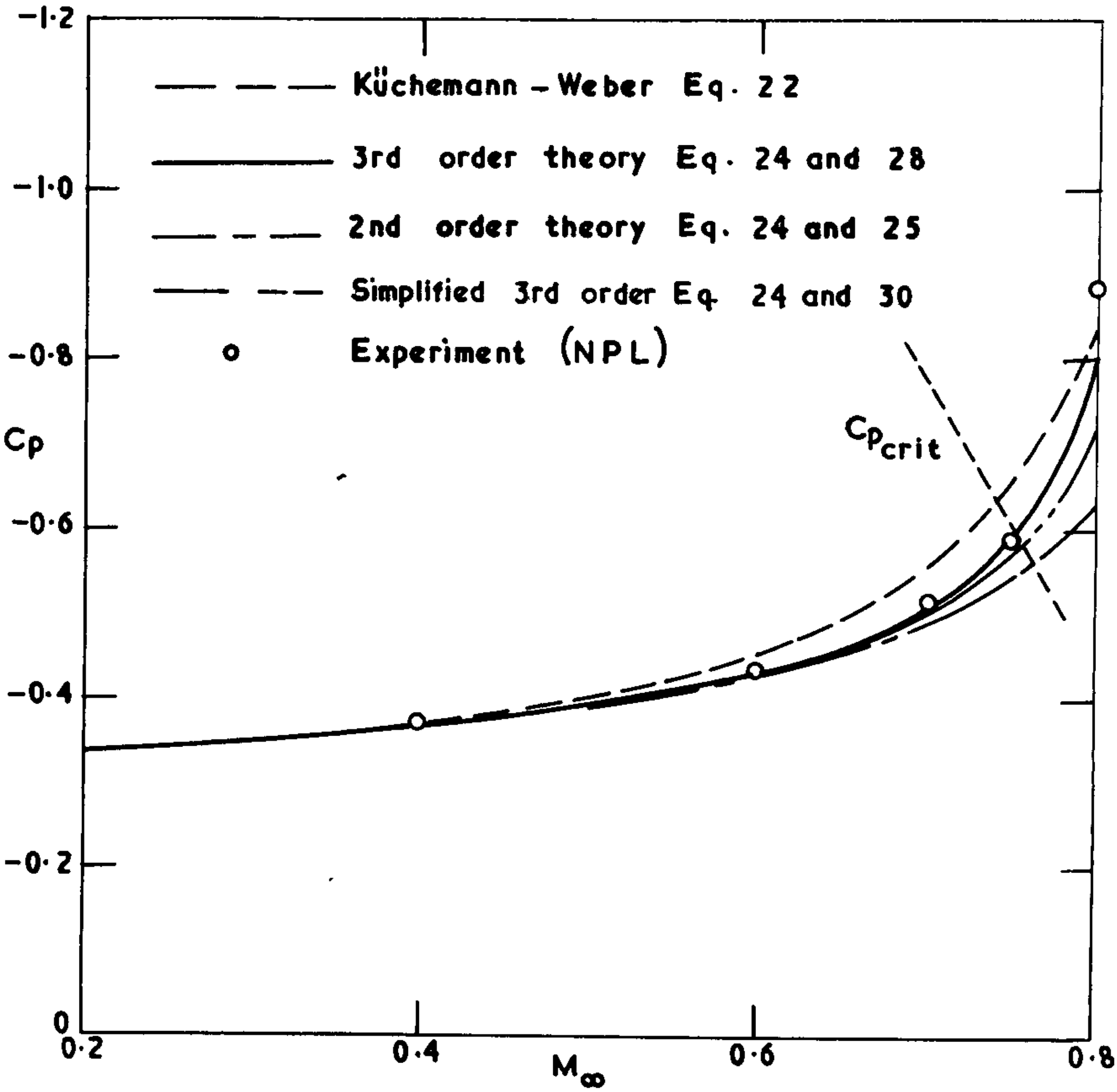

Pressure at crest of a NACA 0012 aerofoil

FIG. 8

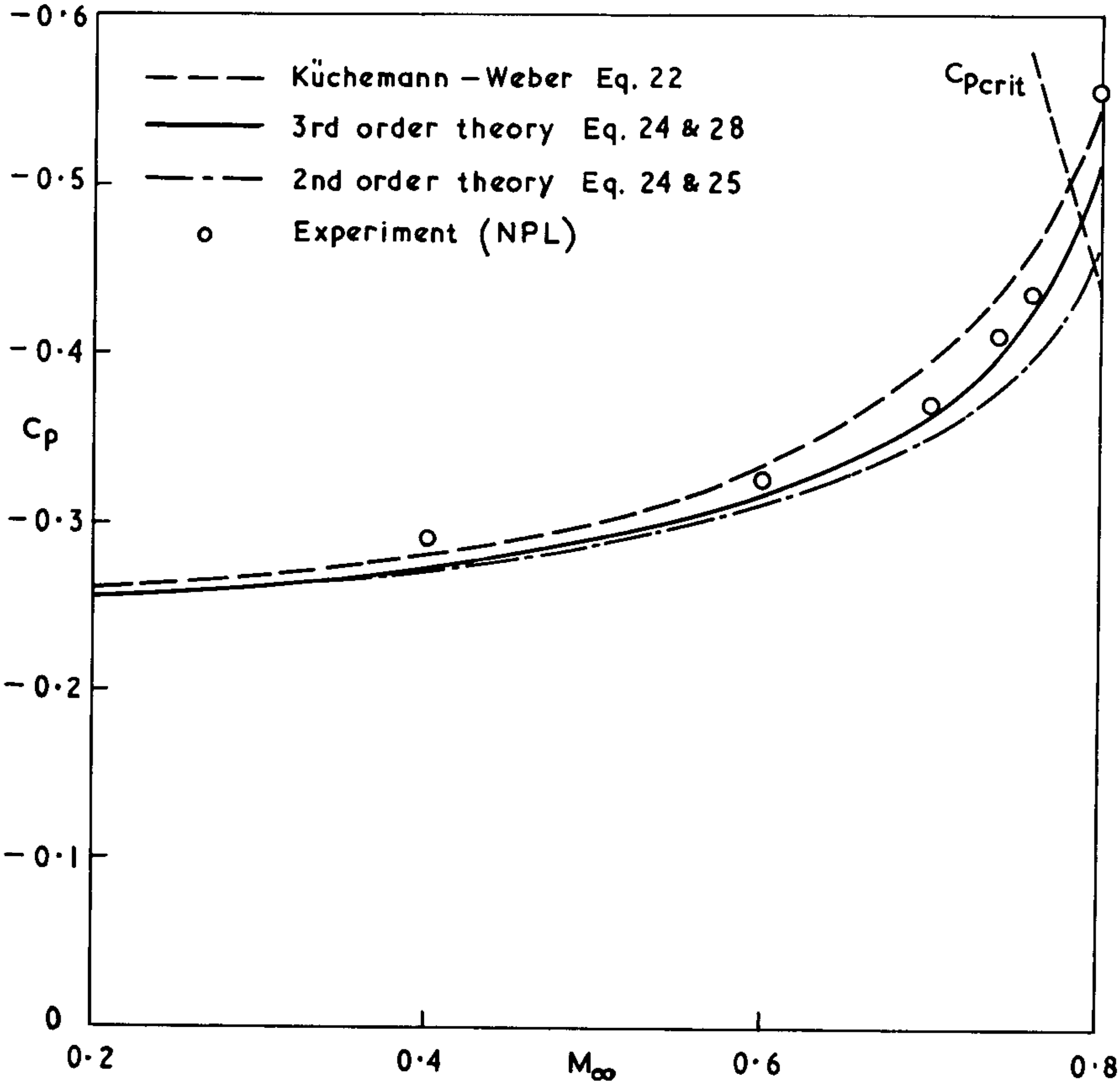

Pressure at crest of a 10% RAE 104 aerofoil

FIG. 9

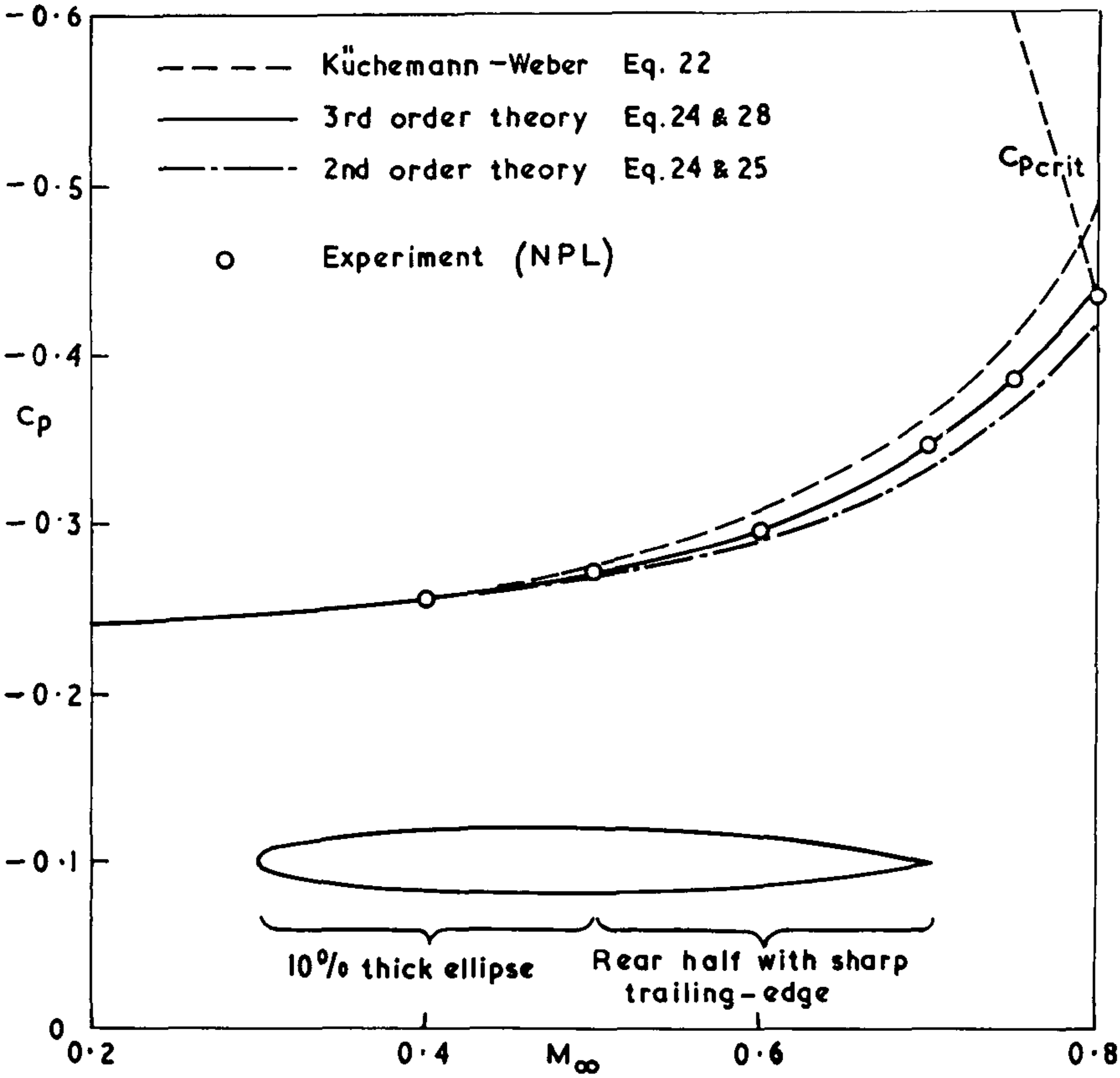

Pressure at crest of a 10% thick elliptic aerofoil

FIG. 10

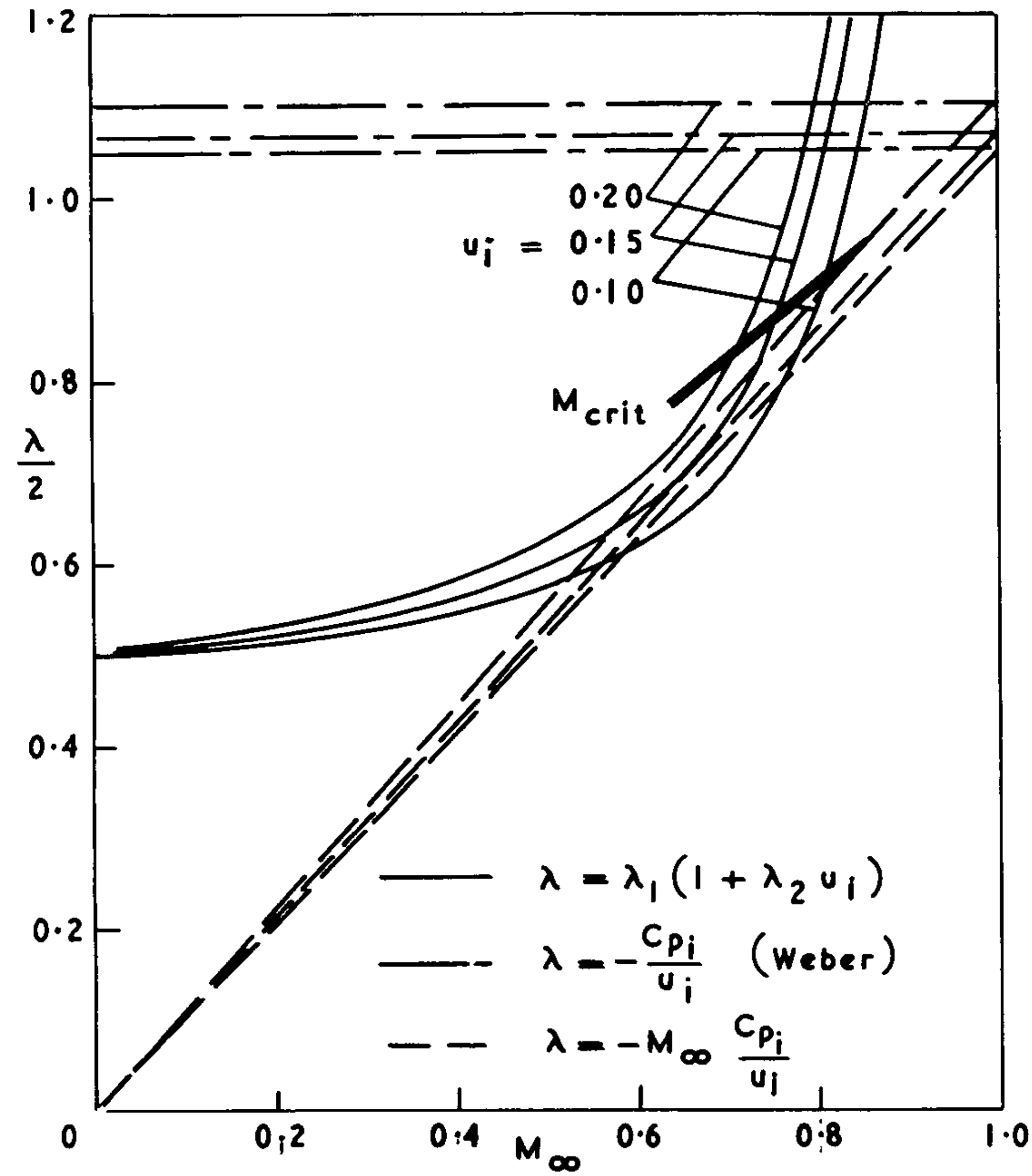

Comparison of various expressions for λ

FIG. 11

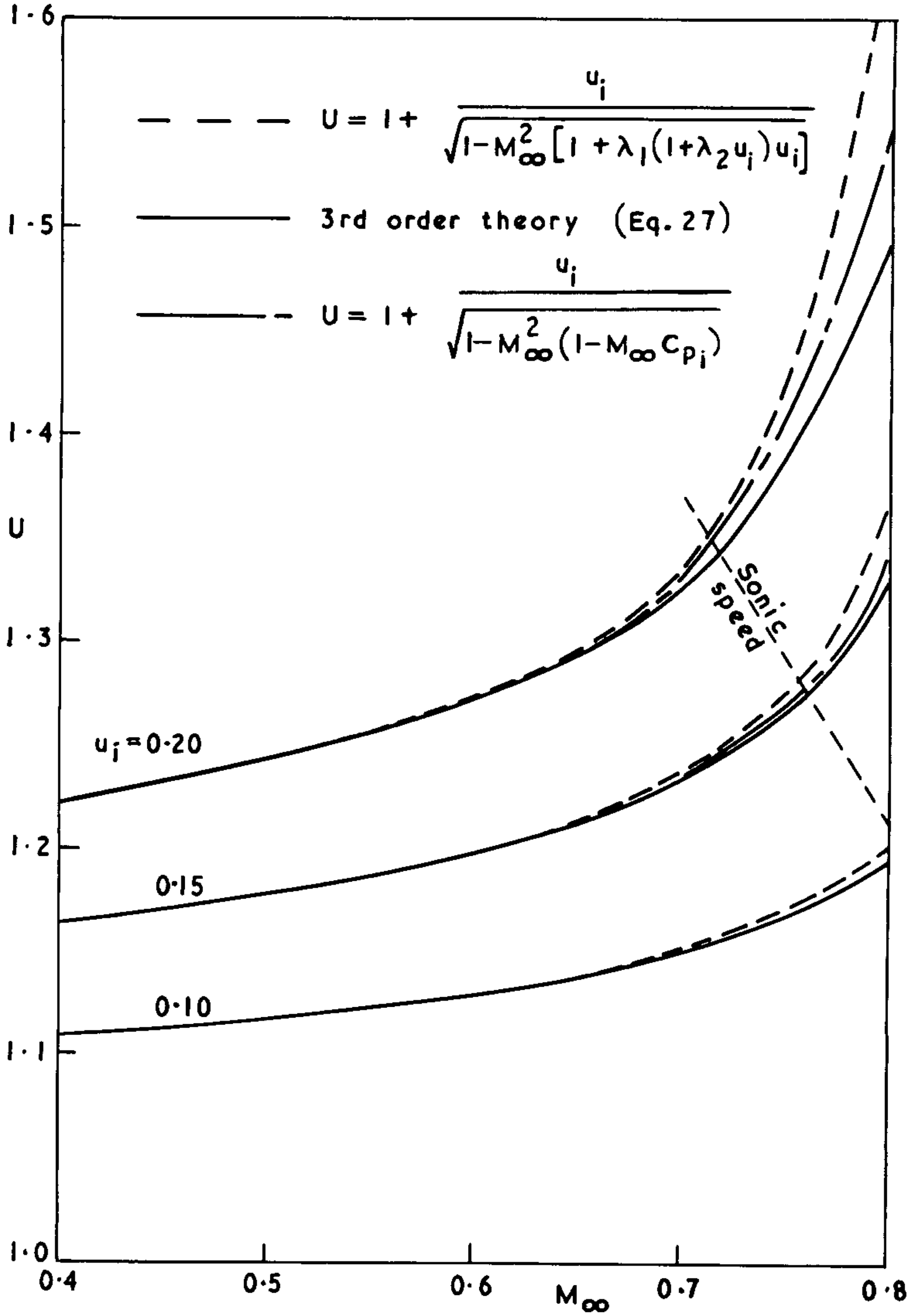

Velocity given by simplified compressibility factor compared with third-order results

FIG. 12

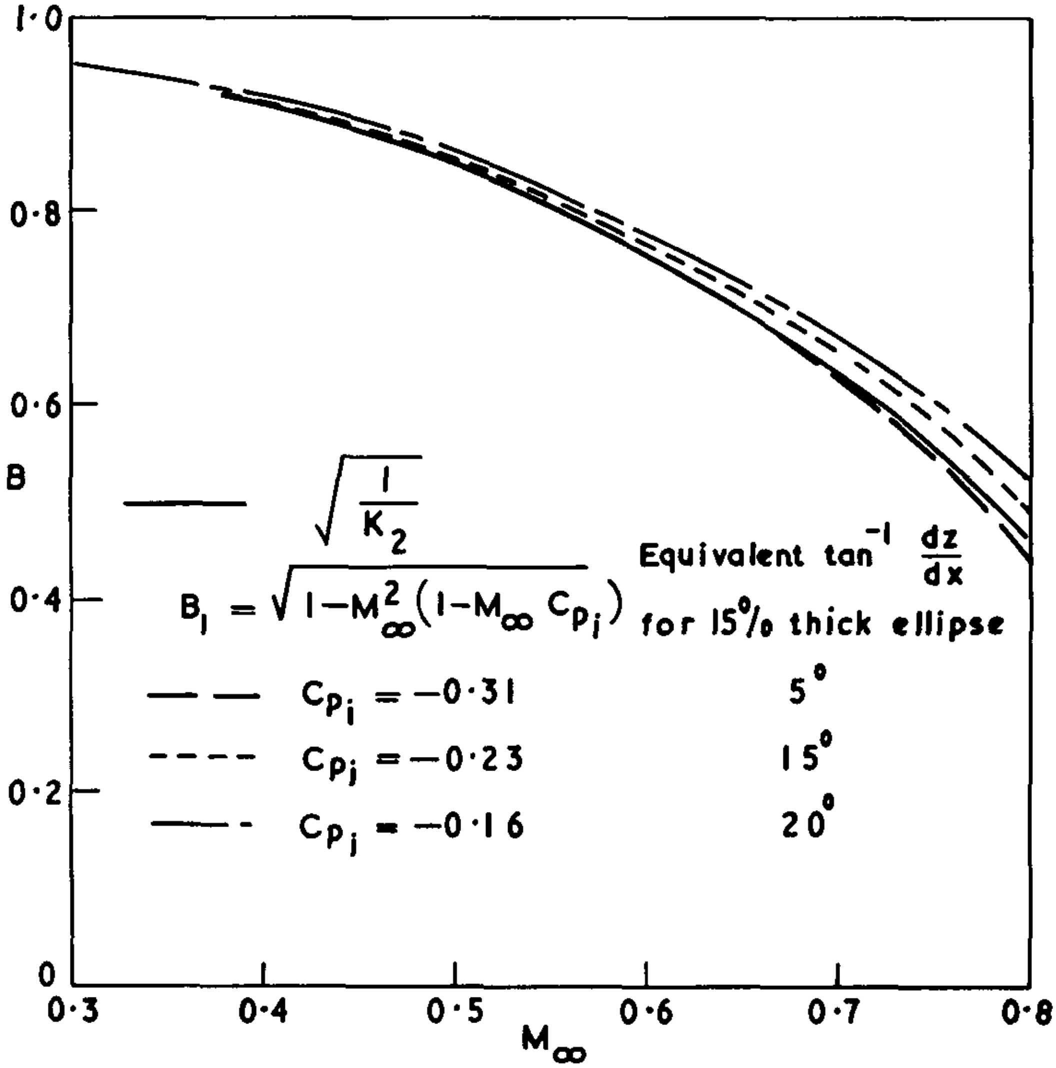

Comparison of two possible compressibility factors for application to the slope term in the Weber formula

FIG. 13

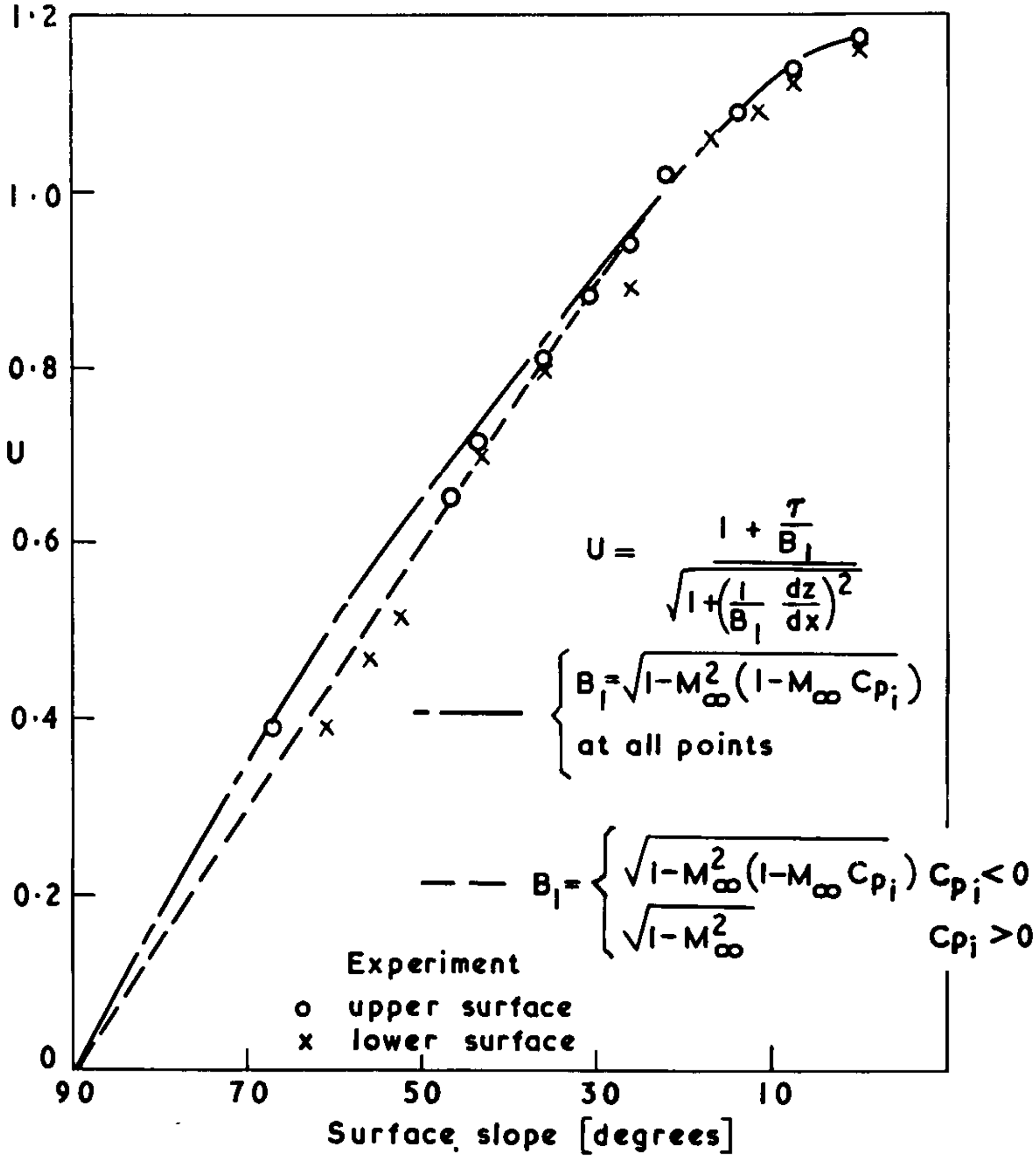

Velocity distribution over the leading edge of a 10% thick elliptic aerofoil at $M = 0{\cdot}4$, $\alpha = 0°$

FIG. 14

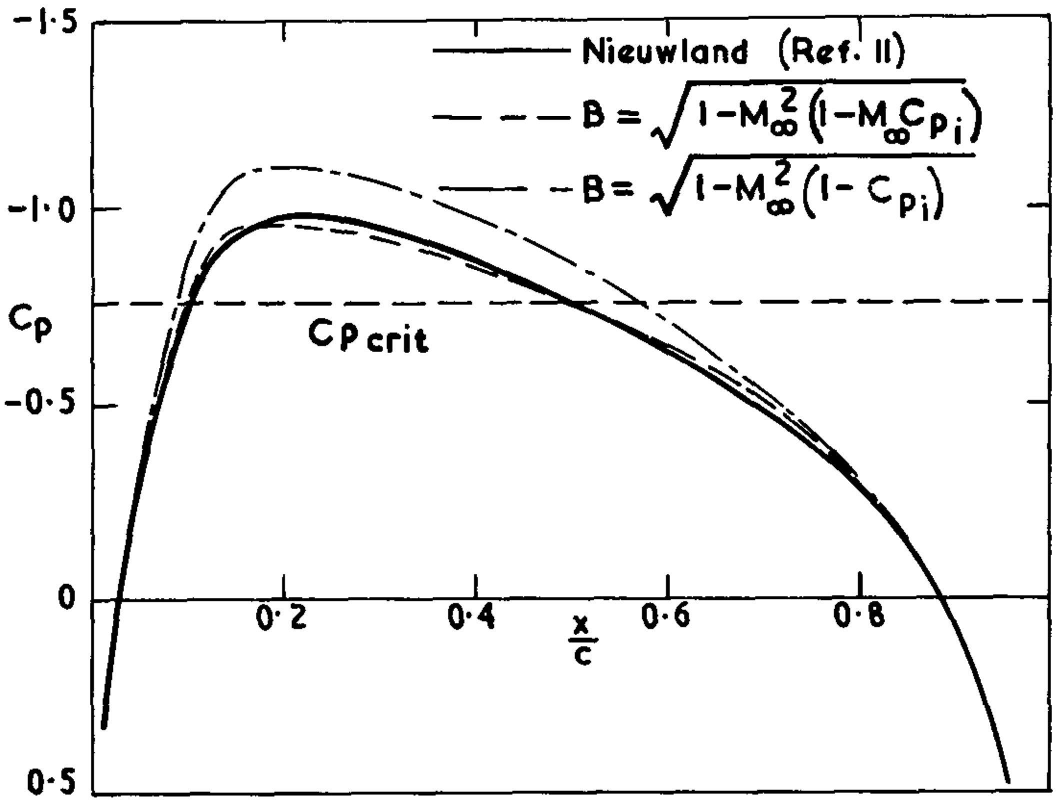

Pressure distribution on a Nieuwland aerofoil (0·09, 0·6, 1·0) at $M_\infty = 0{\cdot}706$, $\alpha = 0^\circ$

FIG. 15

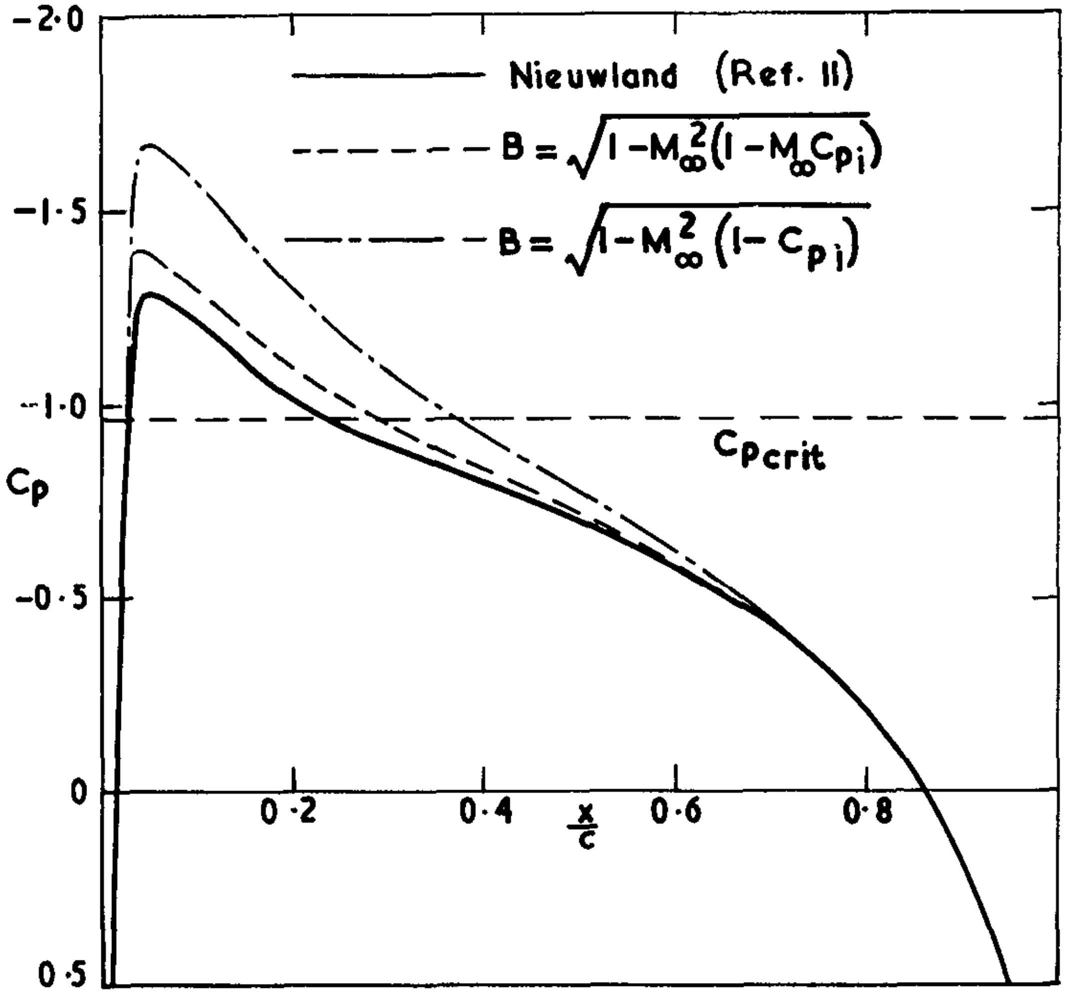

Pressure distribution on a Nieuwland aerofoil (0·08, 0·6, 2·(
at $M_\infty = 0{\cdot}659$, $\alpha = 0^0$

FIG. 16 a

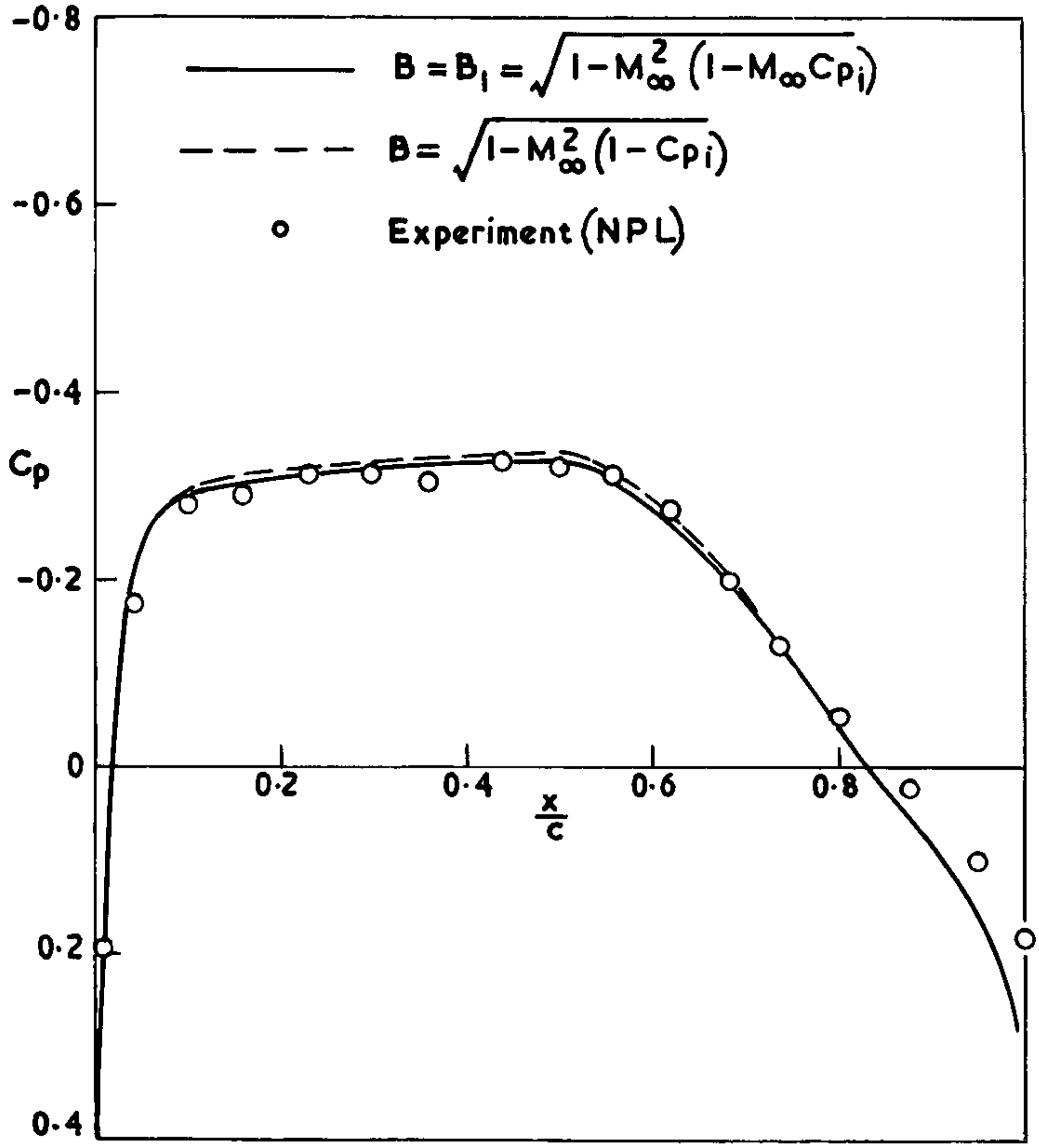

Pressure distribution on 10% thick RAE 104 aerofoil at $M_\infty = 0{\cdot}6$, $\alpha = 0°$

FIG.16 b

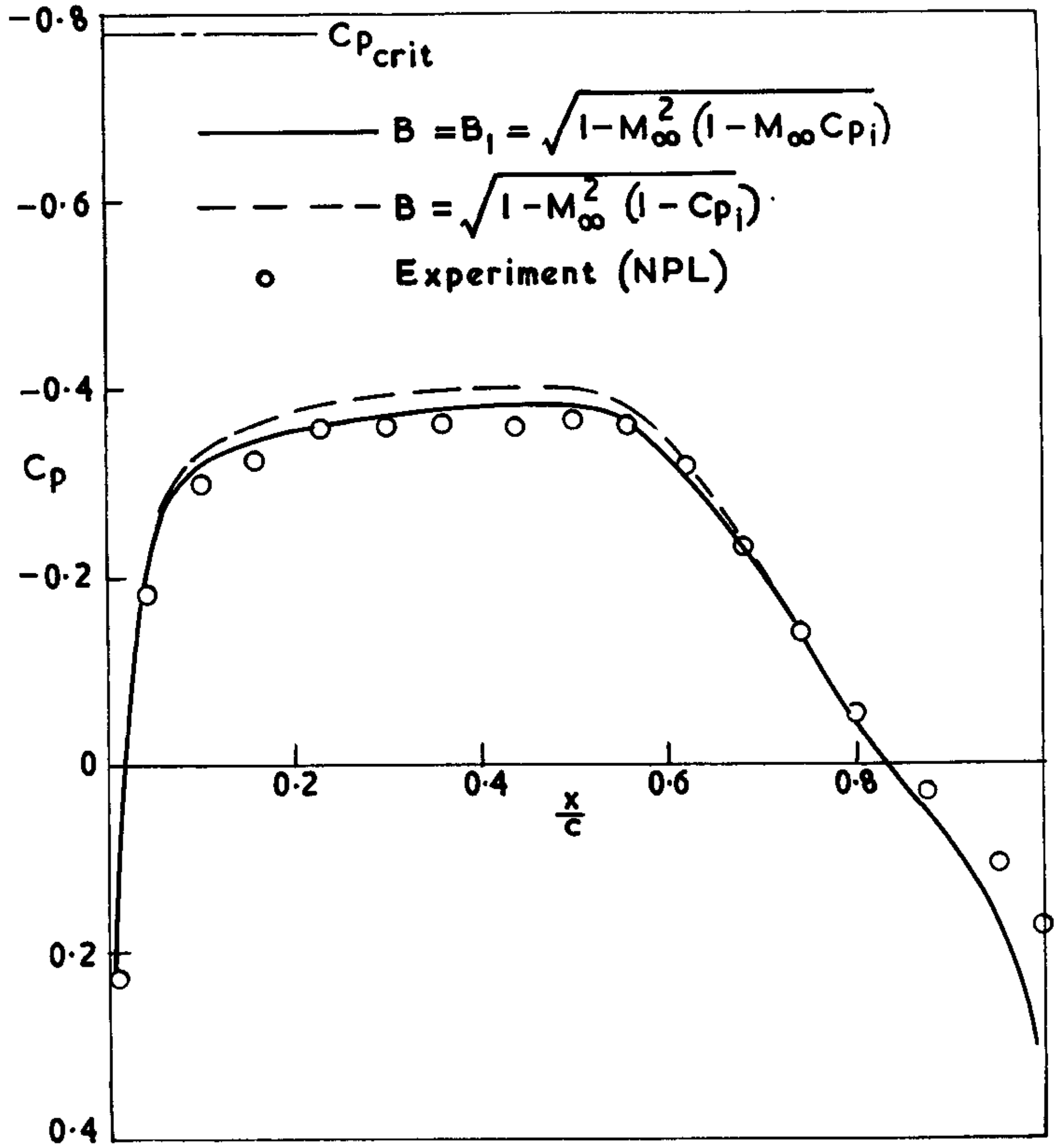

Pressure distribution on 10% thick RAE 104 aerofoil at $M_\infty = 0{\cdot}7$, $\alpha = 0°$

FIG. 16c

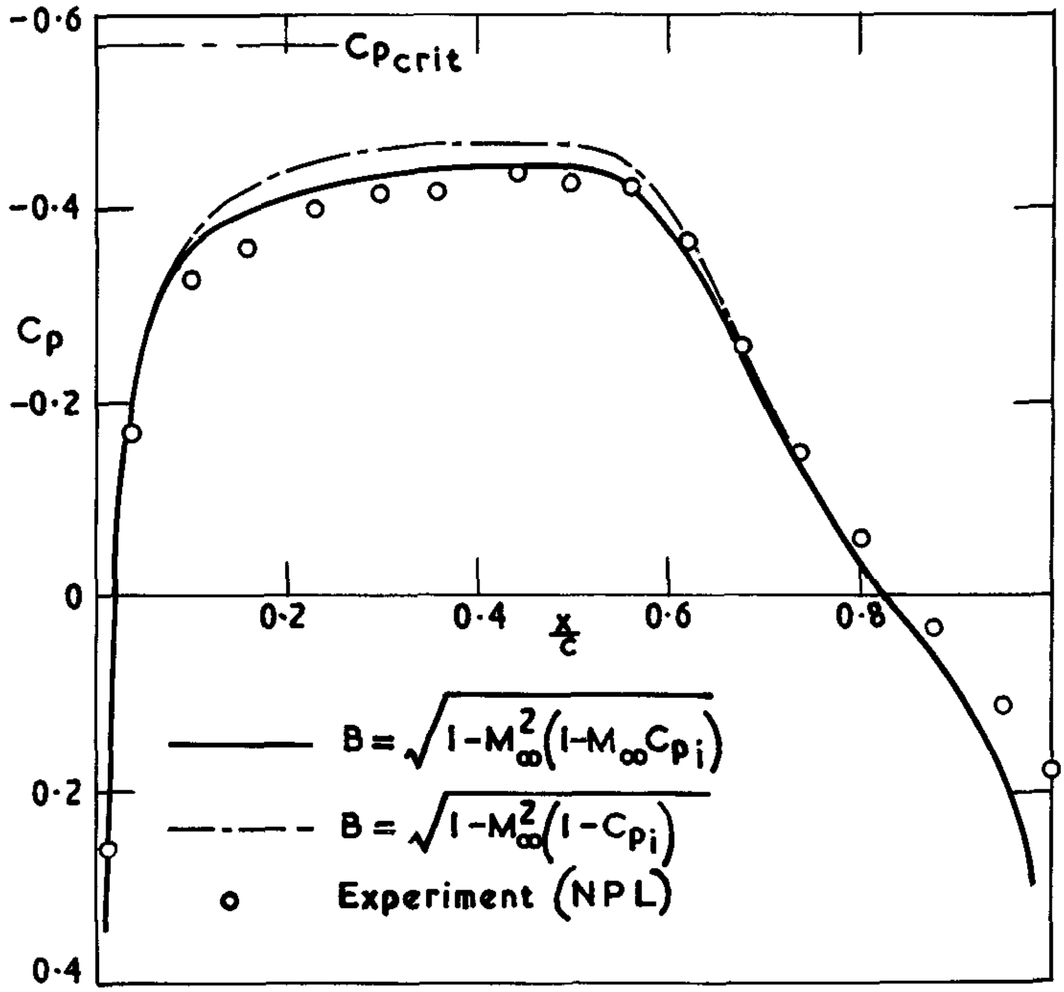

Pressure distribution on a 10% thick RAE 104 aerofoil at $M_\infty = 0{\cdot}76$, $\alpha = 0°$

FIG.17 a

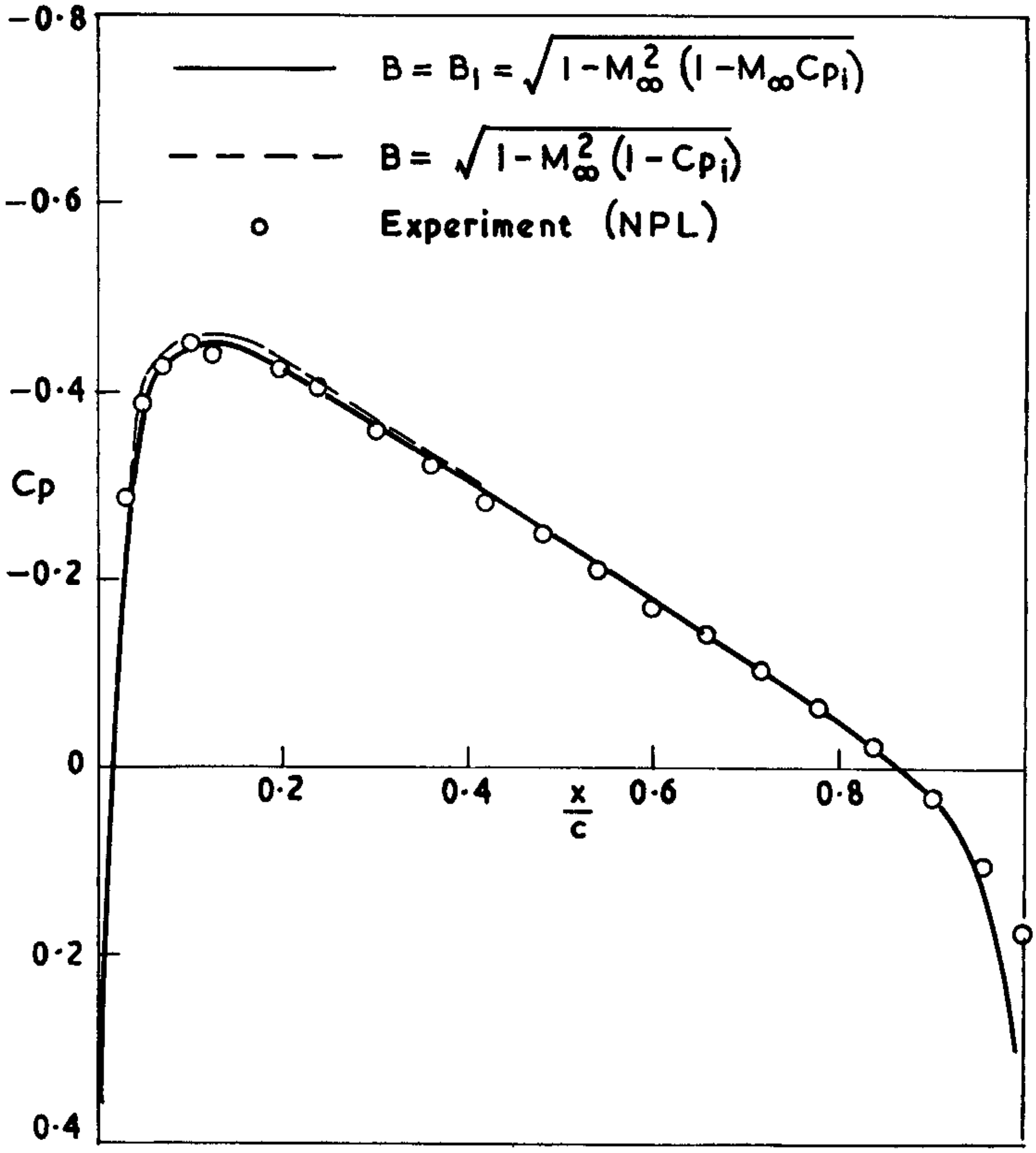

Preasure distribution on NACA 0012 aerofoil

at $M_\infty = 0{\cdot}4,\ \alpha = 0^\circ$

FIG.17 b

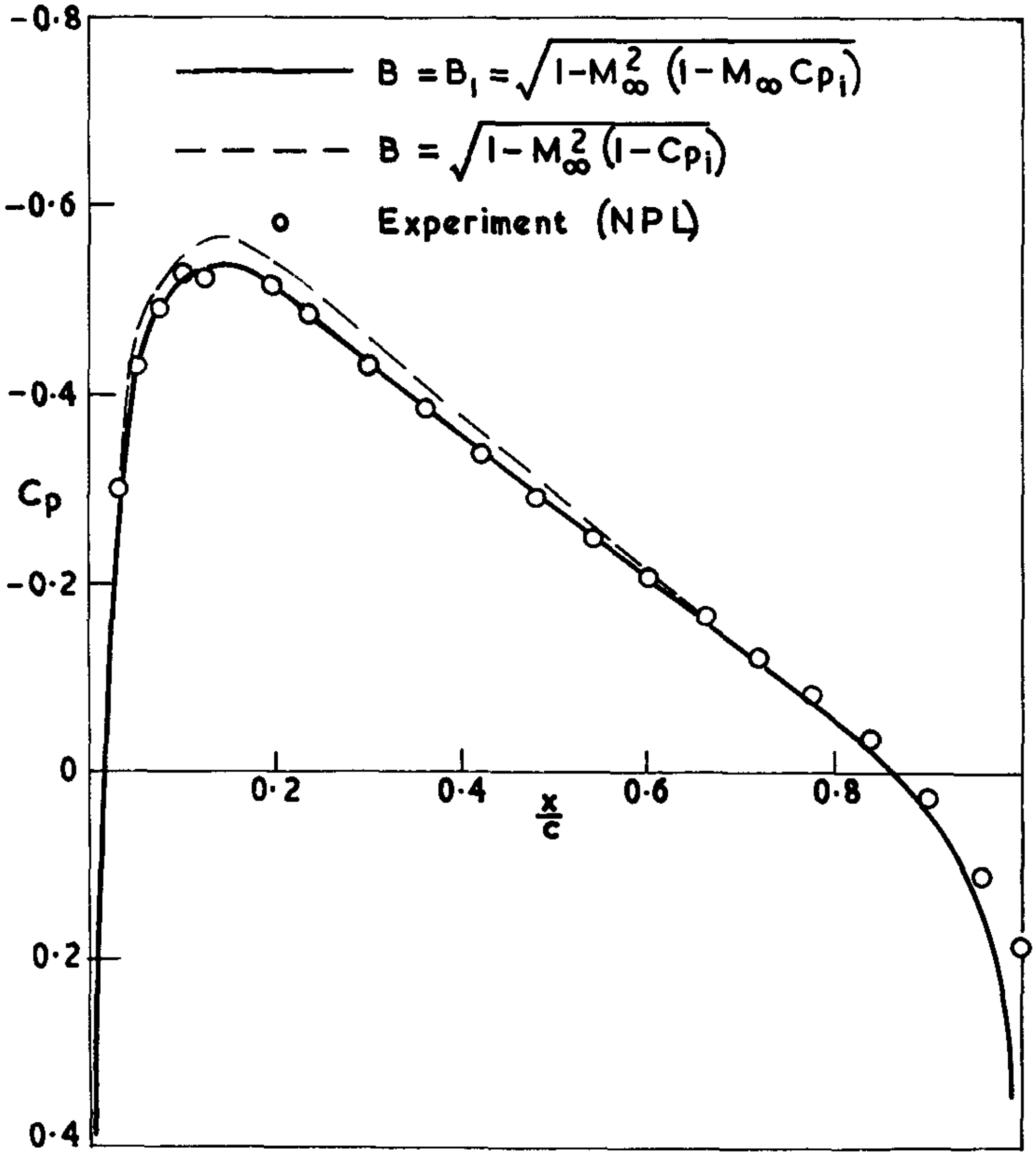

Pressure distribution on NACA 0012 aerofoil at $M_\infty = 0{\cdot}6$, $\alpha = 0°$

FIG. 17 c

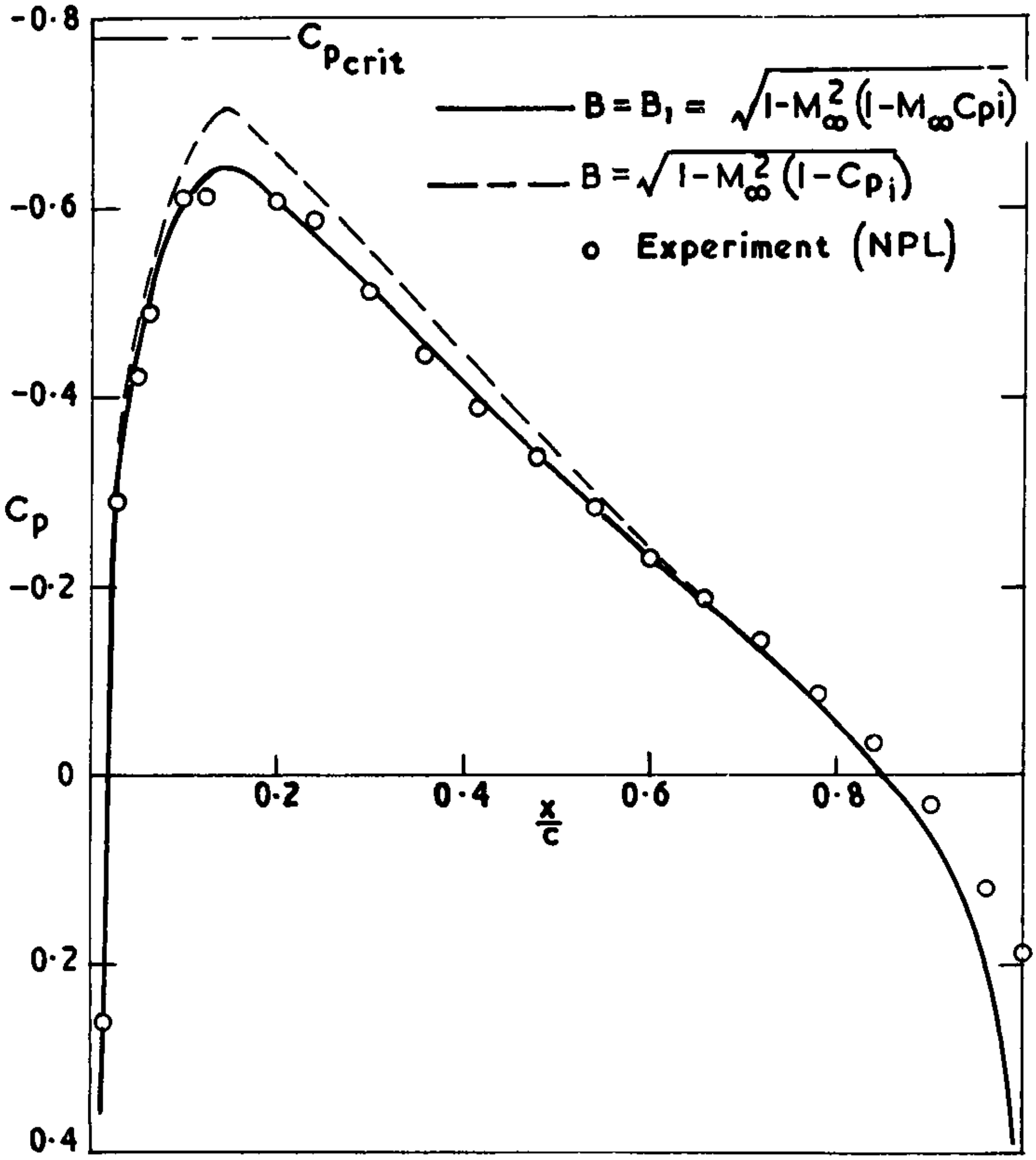

Pressure distribution on NACA 0012 at $M_\infty = 0{\cdot}7, \alpha = 0^0$

D 99238/1/29528 K3 4/68 P CL

A.R.C. C.P. No.993
March, 1967
P. G. Wilby

THE CALCULATION OF SUB-CRITICAL PRESSURE DISTRIBUTIONS ON SYMMETRIC AEROFOILS AT ZERO INCIDENCE

After a review of existing compressibility correction rules a new correction factor is derived using third-order theory. This new factor is used in the calculation of sub-critical pressure distributions on symmetric aerofoils at zero incidence. Theory and experiment are found to agree well.

A.R.C. C.P. No. 993
March, 1967
P. G. Wilby

THE CALCULATION OF SUB-CRITICAL PRESSURE DISTRIBUTIONS ON SYMMETRIC AEROFOILS AT ZERO INCIDENCE

After a review of existing compressibility correction rules a new correction factor is derived using third-order theory. This new factor is used in the calculation of sub-critical pressure distributions on symmetric aerofoils at zero incidence. Theory and experiment are found to agree well.

A.R.C. C.P. No.993
March, 1967

P. G. Wilby

THE CALCULATION OF SUB-CRITICAL PRESSURE DISTRIBUTIONS ON SYMMETRIC AEROFOILS AT ZERO INCIDENCE

After a review of existing compressibility correction rules a new correction factor is derived using third-order theory. This new factor is used in the calculation of sub-critical pressure distributions on symmetric aerofoils at zero incidence. Theory and experiment are found to agree well.

C.P. No. 993

Printed and published by
HER MAJESTY'S STATIONERY OFFICE
To be purchased from
49 High Holborn, London W C 1
423 Oxford Street, London W 1
13A Castle Street, Edinburgh 2
109 St Mary Street, Cardiff CF1 1JW
Brazennose Street, Manchester 2
50 Fairfax Street, Bristol 1
258–259 Broad Street, Birmingham 1
7–11 Linenhall Street, Belfast BT2 8AY
or through any bookseller
Printed in England

C.P. No. 993

S O. Code No 23-9017-93